

## Comparative Histological Study on the Possible Protective Effect of Mitoquinone Versus Oxymatrine on Cerebellar Cortex of Adult Male Albino Rats Treated with Sofosbuvir

Mona A. Soliman, Rania S. Emar and Dalia A Noya

Department of Histology and Cell Biology, Faculty of Medicine, Menoufia University, Egypt

### ABSTRACT

**Introduction:** Chronic hepatitis C is worldwide public-health issue. It is considered main cause for liver-related morbidity and mortality. Sofosbuvir, a direct-acting antiviral drug has revolutionized HCV treatment with high success rate. However, its effect on cerebellum still unclear. Mitoquinone and Oxymatrine have neuroprotective effects.

**Aim of Work:** This study objective was to assess neurological protective benefits of Mitoquinone versus oxymatrine against alterations in cerebellar cortex of adult male albino rats treated with Sofosbuvir.

**Materials and Methods:** Seventy-six adult male wistar albino rats were categorized into six groups, group I served as control group (n=16), group II (n=12) and III (n=12) (Mito Q and oxymatrine treated respectively), IV (n=12) (Sofosbuvir treated group), V (n=12) (Sofosbuvir and Mito Q group) and VI (n=12) (Sofosbuvir and Oxymatrine group). For biochemical, histological, Immunohistochemical (Glial Fibrillary Acidic Protein (GFAP), Inducible Nitric Oxide Synthase (iNOS) and Caspase-3) and electron microscopic evaluations, cerebellum was extracted and processed at the end of study. Also, Morphometric studies had been performed.

**Results:** Sofosbuvir treatment demonstrated altered cerebellar cortex structure. The molecular layer exhibited perineuronal spaces with myelin sheath splitting encircling nerve fibers. Moreover, Purkinje cells lost their Nissl's granules and had a disorganized, shrunken appearance with hyperchromatic nuclei. Small, degenerated granule cells were visible in the granular layer. GFAP, iNOS, and Caspase-3 immunoreaction all showed highly significant increase. Mitoquinone (Mito Q) and oxymatrine administrations improved these alterations. Mitoquinone (Mito Q) displayed greater neuroprotection against histological changes on cerebellar cortex treated with Sofosbuvir.

**Conclusion:** Sofosbuvir treatment causes histological and immuno-histochemical alterations in cerebellar cortex of albino male adult rats. Mitoquinone outperforms oxymatrine as neuroprotective.

**Received:** 01 December 2023, **Accepted:** 05 January 2024

**Key Words:** Cerebellar cortex, mitoquinone, oxymatrine, sofosbuvir.

**Corresponding Author:** Dalia A. Noya, MD, Department of Histology and Cell Biology, Faculty of Medicine, Menoufia University, Egypt, **Tel.:** +20 10 6846 4307, **E-mail:** dalia\_noya@yahoo.com

**ISSN:** 1110-0559, Vol. 48, No. 1

### INTRODUCTION

An infection with Hepatitis C virus (HCV) provides a serious health challenge. It can cause both acute and chronic illness. About fifty-eight million people worldwide suffer from chronic hepatitis C virus infection, and there are two million new cases each year. Adolescents and children with chronic hepatitis C were also, monitored. Most of deaths from hepatitis C were caused from its complications as cirrhosis and hepatocellular carcinoma (HCC)<sup>[1]</sup>.

According to some scientists<sup>[2]</sup> in 2013, Egypt had the highest global rate of HCV prevalence, and in 2017, it had the fifth-highest number of HCV-positive people. At beginning of 2018, roughly 2 million people with active HCV infections were still largely unidentified.

A promising antiviral therapy against numerous genotypes of hepatitis C virus (HCV) is sofosbuvir. Being a nucleotide analog, Sofosbuvir can suppress NS5B polymerase that is needed for HCV viral RNA replication<sup>[3]</sup>. Sofosbuvir is orally administered, well known by its high

tolerance response, low rate of failure, good efficacy, having no major drug-drug interaction with few adverse effects<sup>[4]</sup>.

Unfortunately, previous studies reported some adverse effects associated with Sofosbuvir as gastrointestinal irritation, headache, anemia, insomnia, hair loss, muscle spasm as well as birth defects so it was unrecommended in pregnant female patients<sup>[5]</sup>, renal toxicity<sup>[6]</sup>, lung toxicity<sup>[7]</sup> and corneal changes<sup>[8]</sup>.

The cerebellum is especially vulnerable to various antivirals. An earlier study implied that the receiving of Sofosbuvir caused cerebellar degeneration and structural changes<sup>[4]</sup>. Therefore, despite of being affirmative drug for chronic HCV infection, we need to put the effects of Sofosbuvir on cerebellar cortex in spotlight.

Mitoquinone (Mito Q) is a drug, composed of coenzyme Q10 and triphenyl phosphonium that targets Mitochondria and acts as antioxidant by prevention of mitochondrial dysfunction<sup>[9]</sup>. Mito Q blocks mitochondrial reactive

oxygen species (ROS) that damage cells<sup>[10]</sup>. Additionally, Mito Q beneficial effects was proved in several disorders, such as neurodegenerative disorders, hepatic inflammatory disease, diabetic nephropathy, sepsis, and testicular oxidative damage<sup>[11,12]</sup>.

Chinese herbal medicine is widely used as treatment or prophylaxis in various medical conditions as it has less cost, less adverse effects and sometimes it is easily obtained. Oxymatrine (OMT) is a traditional Chinese herb extracted from *Sophora flavescens* Aiton<sup>[13]</sup>.

Oxymatrine has drawn a great attention because of its beneficial effects on different tissues. It has anti-inflammatory, anti-oxidative stress and anti-fibrotic functions<sup>[14]</sup>. Recent researches revealed neuroprotective impacts of Oxymatrine<sup>[15]</sup>.

So, this work was created to evaluate neuroprotective impacts of mitoquinone (Mito Q) and oxymatrine against histological and immunohistochemical alterations within cerebellar cortex of adult male albino rats treated with Sofosbuvir.

## MATERIALS AND METHODS

### Animals

Seventy-six adult male albino wistar rats weighing  $190 \pm 10$  grams were included in this study. All of which were twelve weeks old. They were kept in wire mesh cages in clean, well-ventilated environment with a regular light-dark cycle. Animals were fed a conventional pelleted meals having unrestricted access to water. The experiment was conducted in compliance with the ethical guidelines of National Institutes of health (NIH) for using animals in research, at Faculty of medicine, Menoufia University, Egypt. This study received Institutional Research Board (IRB) approval (Code number: 9/2023 HIST 6). Animals' general health and behavior were inspected.

### Chemicals

**Sofosbuvir:** Sofosbuvir (Gratisovir®) was purchased from Pharco Pharmaceuticals, Amriya - Alexandria, Egypt; as tablets of 400 mg each.

**Oxymatrine:** (with a purity >98%) was purchased on line as white crystalline powder from Sigma-Aldrich Saint Louis, Missouri, USA.

**Mitoquinone (Mito Q):** was purchased on line from Med Chem Express, HPLC  $\geq 98\%$ , HY-1001 16A, USA; in the form of capsules each of 5mg.

### Experimental protocol

The period of experiment was six weeks. Animals were assigned randomly to six main groups:

**Group I** (control groups) (n=16): which was divided to three sub-groups:

- Control IA (Negative control) (n=6): animals of this group remain untreated.

- Control IB (n=5): 1 ml of distilled water-diluting vehicle for Sofosbuvir and Mito Q- was given to these rats by gastric gavage once daily for six weeks.
- Control IC (n=5): 1ml normal saline (0.9% sodium chloride)- Oxymatrine diluting vehicle- was given to animals by gastric gavage once daily for six weeks.

**Group II** (Mito Q treated group) (n=12): received Mito Q, dissolved in distilled water by gastric gavage, twice weekly for six weeks at a dose of 5mg/kg<sup>[16]</sup>. For six weeks, each rat was given 1 ml of a solution made by stirring five Mito Q capsules after grinding in 25 ml of distilled water twice weekly by gastric gavage.

**Group III** (Oxymatrine treated group) (n=12): received Oxymatrine through gastric gavage at a dose 80 mg/kg/day dissolved in NaCl 0.9% for six weeks<sup>[17]</sup>. Each rat received 1ml from solution made by dissolving 1 gram of oxymatrine in 62.5 ml of NaCl 0.9% through gastric gavage daily during experiment period.

**Group IV** (Sofosbuvir treated group) (n=12): Sofosbuvir was given at 40 mg/kg, per dose once daily for six weeks<sup>[18]</sup>. For six weeks, each animal was given 1ml of solution made by dissolving a tablet (400mg) after its grinding in 50 ml distilled water by gastric gavage once daily.

**Group V** (Sofosbuvir-MitoQ treated group) (n=12): Sofosbuvir, 40 mg/kg body weight per dose daily<sup>[18]</sup> and Mito Q, 5mg/kg body weight per dose twice weekly<sup>[16]</sup> were given during experiment period.

**Group VI** (Sofosbuvir-Oxymatrine treated group) (n=12): Sofosbuvir, 40 mg/kg body weight, per dose daily<sup>[18]</sup> concomitantly with Oxymatrine, 80 mg/kg/day,<sup>[17]</sup> were given during experimental period

At the end of the experiment, Ketamine (90mg/kg)<sup>[19]</sup> was given by intraperitoneal injection to anaesthetize all groups of rats. The specimens were then partially fixed through intra-cardiac perfusion with 2.5% glutaraldehyde in 0.1 mol/L phosphate buffer at pH 7.4. Each rat's cerebellum was carefully removed and separated into two halves for biochemical, histological, and immunohistochemical analysis.

### Biochemical study

cerebellar tissues were extracted, homogenized, and then centrifuged for assessment of oxidant-antioxidant status of the rats by measuring the quantity of malondialdehyde (MDA), along with superoxide dismutase (SOD) and reduced glutathione (GSH) activity within cerebellar tissue. The Yeginsu and Ergin method<sup>[20]</sup>, was used to measure the activity of MDA, expressing its measurements in nanomoles per gram of protein. Reduced glutathione (GSH) was detected using Ganesan *et al.* technique<sup>[21]</sup>, with the results expressed in milligrams per gram of protein. The activity of SOD was determined using

the Lu and Finkel technique<sup>[22]</sup>. Its findings were recorded as protein units per gram.

### Light microscopic study

#### a- Histological study

The right cerebellar tissues halves were fixed for one week in 10% formalin solution. Specimens were cleared, dehydrated, and immersed in paraffin wax then were cut to 5  $\mu$ m thick sections. Haematoxylin and eosin (H and E) stain was applied for demonstration of histological structure of cerebellar cortex<sup>[23]</sup>. Also, toluidine-blue stained sections were examined for presence of Nissl's granules<sup>[24]</sup>.

#### b- Immunohistochemical study

After removal of paraffin from 5  $\mu$ m sections thickness, rehydration and washing with phosphate buffered saline was done. Sections were soaked all night long with the primary antibodies listed below.

Anti-GFAP (Glial Fibrillary Acidic Protein) antibody: mouse monoclonal antibody for GFAP, dilution 1/100, (Sigma, St Louis, Missouri, USA) and a technique involving modified avidin-biotin peroxidase (Thermo Scientific Co, Waltham, Massachusetts, USA) was used to demonstrate fibrillary acidic protein present in intermediate filaments of astrocytes<sup>[25]</sup>. Cytoplasmic brown coloration of astrocytes and their processes was regarded positive. For positive control, brain tissue was applied.

Anti-iNOS (Inducible Nitric Oxide Synthase) antibody (an oxidative stress marker): Immunoperoxidase stain for Inducible Nitric Oxide Synthase (iNOS), dilution 1:200, (BD Biosciences, San Diego, CA) was used to determine (iNOS) in the cytoplasm using Labeled Streptavidin–Biotin immunoperoxidase technique<sup>[26]</sup>. Brown coloration of cytoplasm served as positive reaction. For positive control colon sample was used.

Anti-caspase-3 antibody (an apoptosis indicator): The rabbit polyclonal anti-Caspase-3 antibody, dilution 1:200, (PA1-26426, Abcam, USA) was used as the primary antibody. A positive reaction was defined as brown cytoplasmic coloration. As a positive control, a section of a human tonsil was utilized<sup>[27]</sup>. The same technique was employed to obtain negative controls, but only the primary antibodies were omitted. Finally, Mayer's hematoxylin was implemented to counterstain all immune-stained slides.

Electron Microscopic study: Tissue samples from the left halves of cerebellum were quickly cut into 1x1mm pieces and immediately fixed for three hours at 4°C in 3% glutaraldehyde buffer at pH 7.4, followed by 2 hours in osmium tetroxide 1% in the same buffer. For tissues dehydration, ascending grades of alcohol were used before being embedded in epoxy resin to create semi thin sections that were stained with 1% toluidine blue and examined under light microscope<sup>[28]</sup>. Uranyl acetate and lead citrate were applied to stain ultrathin sections that were examined and photographed using transmission electron microscope TEM (JEOL, JEM-2100, Tokyo, Japan)<sup>[29]</sup> at the Faculty of Science, Alexandria University, Alexandria, Egypt.

Morphometric and statistical study: For quantitative assessment, 10 different sections from ten different animals in each group were measured by a Leica DML B2/11888111 microscope equipped with a Leica DFC450 camera. Image J software version K1.45 was used to calculate the measured variance. The results were collected from H. and E., Toluidine-blue stained, and immunohistochemistry sections. The following parameters were calculated for quantitative evaluation:

- Mean number of Purkinje cells with H. and E.-stained sections (x 400).
- Mean diameter of Purkinje cells with Toluidine-blue stained sections (x1000)
- Mean thickness of molecular layer of cerebellar cortex in H. and E.-stained sections ( $\times$ 200).
- Mean thickness of granular layer of cerebellar cortex in H. and E.-stained sections ( $\times$ 200).
- Mean area percentage of GFAP immuno-positive reaction in GFAP immuno-stained sections ( $\times$ 200).
- Mean area percentage of iNOS immuno-positive reaction in iNOS immuno-stained sections ( $\times$ 400).
- Mean area percentage of caspase-3 immuno-positive reaction in caspase-3 immuno-stained sections(x400).

All these measurements were set at Faculty of Medicine, Menoufia University, Egypt in Anatomy and Embryology Department.

Statistical analysis: Biochemical and morphometric results of all tested groups were represented as mean  $\pm$  standard deviation (SD), statistically evaluated by SPSS software (version 20) (SPSS, Inc., Chicago, IL, USA). One-way variance analysis (ANOVA) and the Bonferroni's post-hoc test were used to compare data. Results were tabulated and graphed. With, *P* value < 0.05, results were judged statistically significant<sup>[30]</sup>.

## RESULTS

### General observations

- The animals showed normal attitude, appetite and behaviour. Four rats' deaths were reported during experiment.
- All control subgroups were combined to form the control group (I) as a result of their identical histological, immune-histochemical, and morphometrical results.
- group II and group III displayed findings as same as the control group (I) in histological, immune-histochemical, and morphometric evaluations.

### Biochemical results

As regarding mean value ofMDA, group IV (Sofosbuvir treated group) showed high significant rise (*P*<0.001)

in comparison to group I (control group). Group VI (Sofosbuvir- Oxymatrine treated group) was significantly higher ( $P<0.05$ ) in mean value of MDA than group I (control group) and highly significant lower ( $P<0.001$ ) than group IV. However, group V (Sofosbuvir- MitoQ treated group) reviewed non-significant alteration in this parameter ( $P>0.05$ ) when compared to control rats, highly significant decrease ( $P<0.001$ ) in comparison to group IV and decrease ( $P<0.05$ ) in comparison to group VI.

Mean value of GSH and SOD levels exhibited high significant reduction ( $P<0.001$ ) with group IV (Sofosbuvir treated group) in comparison to group I (control group). Group VI (Sofosbuvir- Oxymatrine treated group) revealed significant rise ( $P<0.05$ ) in these variables when compared to group I (control group) and highly significant rise ( $P<0.001$ ) in comparison with group IV. However, group V (Sofosbuvir- MitoQ treated group) showed non-significant alteration in these variables ( $P>0.05$ ) compared to control rats, highly significant elevation ( $P<0.001$ ) in mean value of GSH and SOD as compared with group IV and significant rise ( $P<0.05$ ) in comparison with group VI.

All these data were settled in (Table I, Histogram I).

### Light Microscopic results

#### Histological results

Hx. and E. stained cerebellar sections from control groups (I, II and III) showed normal histological structure. The cerebellum consisted of outer gray matter (cerebellar cortex) with characteristic three layers of neurons; molecular layer, granular layer and Purkinje cell layer in between. Whereas the inner white matter (medulla) was mainly formed of myelinated nerve fibers (Figure 1a). Outer molecular layer contained few parted cells with many nerve fibers. The Purkinje cell layer consisted of a layer of large, pyriform cells with relatively large nuclei arranged in a line at the interface of the molecular layer with the granular layer. Purkinje cells exhibited apical dendritic extensions towards molecular layer. Their cytoplasm houses plenty of basophilic granules (Nissl's granules). Round deeply stained granule cells are packed within the granular layer (Figure 1b).

Cerebellar cortical sections of group IV (sofosbuvir-treated group) showed wide perineuronal spaces around the molecular layer cells. Purkinje layer had disorganized, shrunken cells with small hyperchromatic nuclei. Some cells had deeply stained basophilic cytoplasm while others showed loss of Nissl's granules with vacuolated (empty) neuropil. Intracytoplasmic vacuolation were also, noticed. Empty spaces appeared between cells of the granular layer that also housed some dark shrunken nuclei (Figures 1c,d,e). Vascular congestion and extravasation of blood in different cortical layers were also, noticed (Figure 1f).

Sections of group V (Sofosbuvir and mito Q treated group) displayed nearly normal histological architecture the same as control group with clearly defined Purkinje

cells and poorly defined perineuronal spaces in the molecular cell layer. Moreover, apparently normal closely packed granular cells were noticed within granular layer (Figure 1g).

While, examination of sections from group VI (Sofosbuvir and oxymatrine treated group) revealed nearly normal histological structure of cerebellar cortex. Some Purkinje cells appeared shrunken surrounded with perineuronal spaces. Multiple vacuolations were noticed between cells of molecular layer (Figure 1h).

Cerebellar cortical sections from control groups (I, II, and III) stained with Toluidine blue showed Purkinje cells having vesicular central nuclei and prominent nucleoli. Their cytoplasm was studded with darkly stained Nissl's granules. Bergmann astrocytes with pale-stained nuclei were seen around them. Crowded granular cells with darkly stained nuclei were also, recognized (Figure 2a).

While in Toluidine blue stained cerebellar cortical sections of group IV (sofosbuvir-treated group), Purkinje cells were shrunken having irregular small nuclei. Depletion of its cytoplasmic Nissl's granules were noticed. Purkinje cells were surrounded by small spaces and vacuoles (Figure 2b).

Examination of group V (Sofosbuvir and mito Q treated group) revealed regularly arranged Purkinje cells having vesicular central nuclei. Cytoplasm was studded with Nissl's granules (Figure 2c). While, cerebellar cortical sections of group VI (Sofosbuvir and oxymatrine treated group) exhibited some Purkinje cells with vesicular nuclei and granular cytoplasm. Others displayed small irregular nuclei with granular cytoplasm (Figure 2d).

#### Immunohistochemical results

##### 1- Glial Fibrillary Acidic Protein (GFAP)

Control groups (I, II, III) revealed mild positive immunoreaction within few scattered positive small sized astrocytes having short processes in the molecular and granular layers of cerebellar cortex for Glial Fibrillary Acidic Protein (GFAP) immunohistochemical staining (Figure 3a). Sofosbuvir treated group (IV) showed strong positive immune reaction of GFAP within astrocytes compared to control group (Figure 3b). Mild to moderate immunoreaction for GFAP was observed with Cerebellar cortical sections of group V (Sofosbuvir and mito Q treated group) (Figure 3c). While group VI (Sofosbuvir and oxymatrine treated group) expressed moderate immunoreaction for GFAP (Figure 3d).

##### 2- Inducible Nitric Oxide Synthase (iNOS)

On examination of cerebellar cortical sections of control groups (I, II, III) exhibited negative reaction for iNOS in molecular, Purkinje and granular cell layers (Figure 4a). Strong, positive immunoreaction for iNOS within Purkinje cells as brown cytoplasmic staining was noticed in group IV (Sofosbuvir treated group) (Figure 4b). There was negative to mild iNOS expression in group V

(Sofosbuvir and mito Q treated group) (Figure 4c). While group VI (Sofosbuvir and oxymatrine treated group) revealed moderate immunoreaction for iNOS (Figure 4d).

### 3- Caspase-3 immunostaining

Control groups (I, II, III) revealed negative cytoplasmic immunoreaction within cerebellar cortical sections for Caspase-3 (Figure 5a). Obvious positive immunoreaction of caspase-3 was detected within cytoplasm of Purkinje and granule cells of cerebellar cortical sections of group IV (Sofosbuvir treated group) (Figure 5b) as compared to control group. However, group V (Sofosbuvir and mito Q treated group) showed negative to weak positive immunoreaction within most of Purkinje and granule cells cytoplasm (Figure 5c). While cerebellar cortical sections of group VI (Sofosbuvir and oxymatrine treated group) demonstrated moderate positive cytoplasmic immunoreaction of caspase-3 within Purkinje cells and negative reaction in granule cells (Figure 5d).

### Electron Microscopic results

Control groups (I, II, and III) demonstrated normal standard configuration of cerebellar cortex on examination of ultrathin sections. Several myelinated nerve fibers with varying sizes surrounded by intact myelin sheaths having compact lamellar shape were visible within the molecular layer. Mitochondria and microtubules were present in their axoplasm (Figure 6). Purkinje cell had euchromatic nucleus with prominent nucleolus. Numerous rough endoplasmic reticulum cisternae, Golgi apparatus, scattered free ribosomes, and numerous Mitochondria were found in its cytoplasm (Figure 7). Closely packed granule cells having nuclei containing peripheral clumps of heterochromatin surrounded by thin rim of cytoplasm having mitochondria and free ribosomes occupied granule layer (Figure 8).

On the other hand, group IV (Sofosbuvir treated group) exhibited structural alterations. There was irregularity and splitting of myelin sheath surrounding myelinated nerve fibers within molecular layer with loss of their lamellar compact structure. Their axoplasm was rarified and housed swollen Mitochondria with disrupted cristae. Areas with empty neuropil were noticed (Figure 9). Purkinje cell had irregular heterochromatic nucleus. Several dilated rough endoplasmic reticulum cisternae, disrupted Golgi apparatus, second lysosomes, and disrupted Mitochondria were all found in the cytoplasm. The surrounding neuropil was rarified having several myelinated nerve fibers with thin abnormal myelin sheath (Figure 10). Granular layer revealed cells having irregular, shrunken heterochromatic nuclei with widened perinuclear space. Some cells showed rarified cytoplasm. Irregular thin myelin sheaths surrounded nearby myelinated axons. Empty neuropil and dilated blood vessel were also, demonstrated (Figure 11).

However, group V (Sofosbuvir and mito Q treated group) demonstrated cerebellar cortex structure preservation. Myelinated nerve fibers within molecular layer were surrounded by regular thick continuous myelin sheaths.

Normally appeared neurotubules and Mitochondria were noticed within their axoplasm (Figure 12). The Purkinje cell displayed euchromatic nucleus. Multiple rough endoplasmic reticulum cisternae, Mitochondria and dispersed ribosomes were observed within its cytoplasm (Figure 13). Granular cell layers were occupied with euchromatic nuclei of closely packed cells (Figure 14).

Group VI (Sofosbuvir and oxymatrine treated group) cerebellar cortical sections showed molecular layer having myelinated nerve fibers surrounded by slightly irregular, partially separated myelin sheath. Their axoplasm appeared rarified with disrupted Mitochondria with distorted cristae (Figure 15). The Purkinje cell had euchromatic nucleus. However, some dilated rough endoplasmic reticulum cisternae and swollen mitochondria with destroyed cristae were observed within cytoplasm. Areas of surrounding neuropil appeared empty (Figure 16). Cells of granular layer displayed rounded regularly outlined heterochromatic nuclei. One cell had dark irregular nucleus with wide perinuclear space. The nearby myelinated axons showed normal regular intact myelin sheath with normal appearance of their axoplasm having Mitochondria (Figure 17).

### Morphometrical results

Group IV (Sofosbuvir treated group) demonstrated highly significant reduction ( $P < 0.001$ ) in thickness of molecular and granular layer, diameter and number of Purkinje cells compared with control animals (groups I, II and III). While, group VI (Sofosbuvir- Oxymatrine treated group) displayed significant decrease ( $P < 0.05$ ) in these parameters compared with control animals and highly significant increase ( $P < 0.001$ ) compared with group IV (Sofosbuvir treated group). However, group V (Sofosbuvir- Mito Q treated group) revealed non-significant ( $P > 0.05$ ) alterations in these parameters ( $P > 0.05$ ) as compared with control group, highly significant rise ( $P < 0.001$ ) compared with group IV (Sofosbuvir treated group) and significant rise ( $P < 0.05$ ) in these parameters compared with group VI (Sofosbuvir- Oxymatrine treated group).

All data was settled in (Table 2, Histograms, 2A,B,C).

Group IV (Sofosbuvir treated group) showed highly significant elevation ( $P < 0.001$ ) in mean area percentage of GFAP, iNOS and Caspase-3 in immune-stained sections compared to control animals (group I). On the other hand, group VI (Sofosbuvir- Oxymatrine treated group) displayed significant rise ( $P < 0.05$ ) in these parameters compared to control animals (group I) and highly significant decrease ( $P < 0.001$ ) in comparison with group IV (Sofosbuvir treated group). However, group V (Sofosbuvir- MitoQ treated group) exhibited non-significant ( $P > 0.05$ ) difference in these parameters in comparison to control group (group I), highly significant reduction ( $P < 0.001$ ) compared to group IV (Sofosbuvir treated group) and significant reduction ( $P < 0.05$ ) in these parameters compared to group VI (Sofosbuvir- Oxymatrine treated group).

All data was settled in (Table 3, Histograms, 3A,B,C).

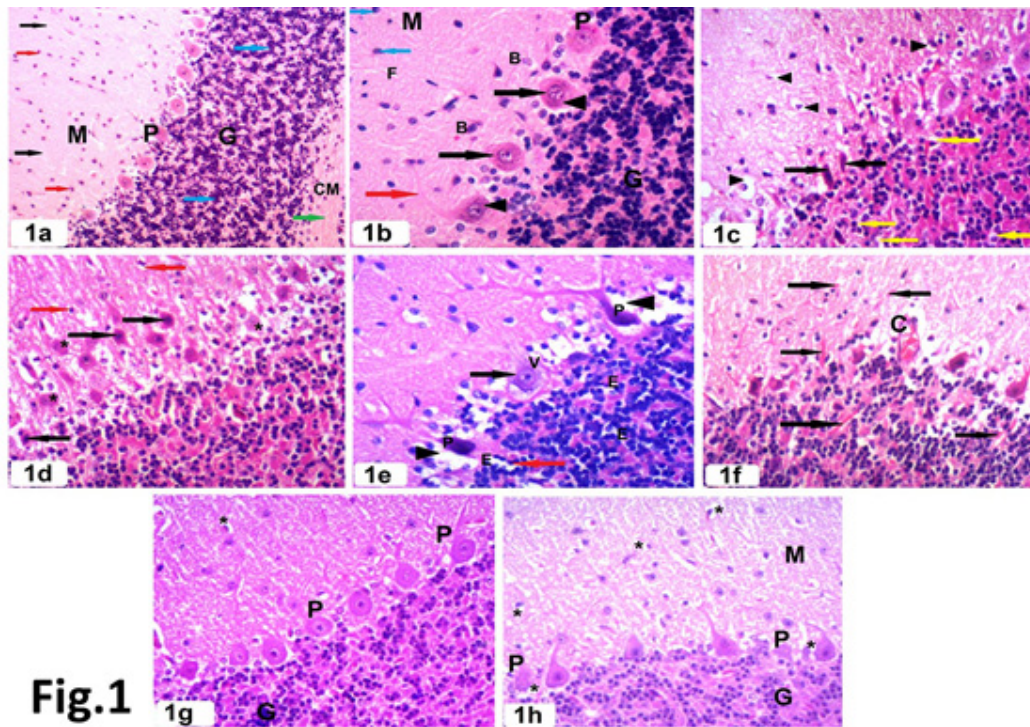


**Fig.1**

**Fig. 1:** Photomicrographs of cerebellar cortex (1a) group I demonstrating three layers of cerebellar cortex [molecular layer (M) contains few cells (red arrow) and plenty nerve fibers (black arrow), granular layer (G) formed of rounded deeply stained closely packed granular cells (blue arrow), Purkinje cell layer (P) with pyriform large cells]. Cerebellar medulla (CM) is formed of myelinated nerve fibers (green arrow) x100. (1b) group I showing deep basket cells (B) and superficial stellate cells (blue arrow) among nerve fibers (F) within molecular layer (M). Large pyriform Purkinje cells with relatively large nuclei arranged in a single row (black arrow) make up Purkinje cell layer (P). Apical dendritic extensions (red arrow) & basophilic granules (Nissl's granules) (▶) are seen in cytoplasm of Purkinje cells. Rounded and intensely stained cells abound in granular layer (G) x400. (1c) group (IV) displaying small hyperchromatic nuclei (black arrow) of Purkinje cells that have shrunken. There are empty spaces between granular layer cells (yellow arrow) and widened perineuronal spaces surrounding cells of molecular layer (▶) x200. (1d) group (IV) demonstrating perinuclear haloes (red arrow) in molecular cells. Purkinje cells are disorganized (\*). Some Purkinje cells exhibits dark nuclei (black arrow) x200. (1e) group (IV) demonstrating some dark Purkinje cells with deeply stained basophilic cytoplasm (P), while others lost their Nissl's granules (black arrow) and surrounded by vacuolated (empty) neuropil (▶). Intracytoplasmic vacuolation (V) are also noticed. Empty spaces (E) are present in-between cells of the granular layer that also houses some dark shrunken nuclei (red arrow) x400. (1f) group (IV) pointing to vascular congestion (C) and extravasation of blood in different cortical layers (black arrow) x200. (1g) group (V) demonstrating molecular layer formed of plenty of nerve fibers with few perineuronal spaces (\*). Pyriform shaped Purkinje cells (P) having oval vesicular nuclei are positioned in a row. Closely packed rounded granular cells (G) occupies granular layer x200. (1h) Group (VI) demonstrating molecular layer (M) with abundant nerve fibers and few cells with persistence of perinural spaces(\*). Some shrunken Purkinje cells (P) and perinural spaces (\*) are present among large pyriform linear arranged ones in Purkinje layer. Rounded crowded granule cells are forming the granular layer (G) x200

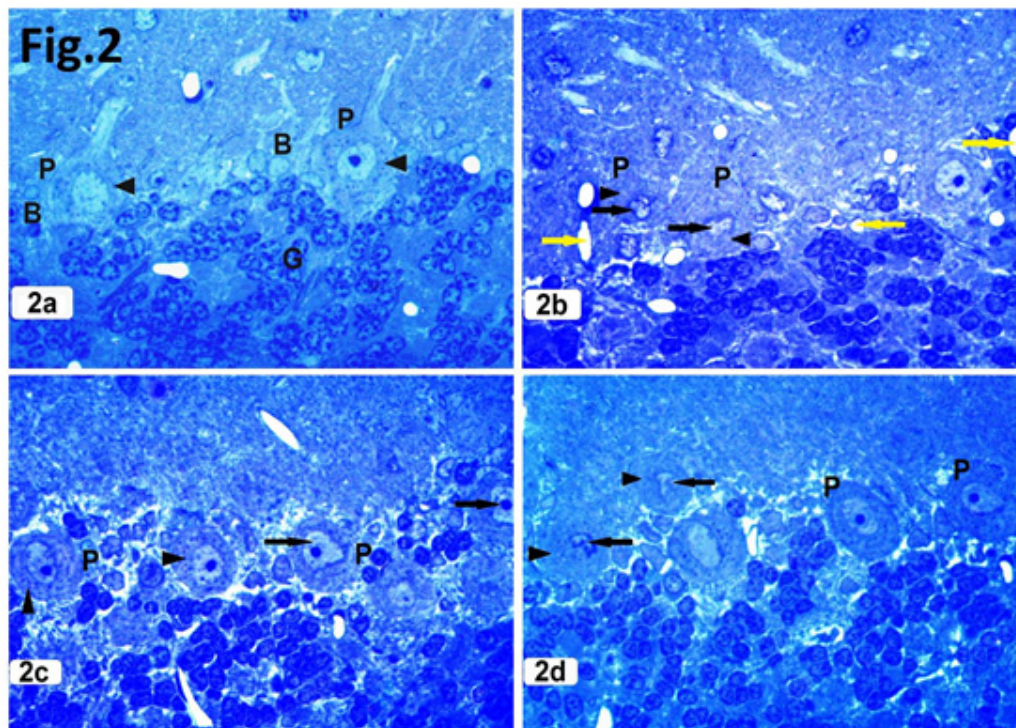


**Fig. 2:** Photomicrographs of toluidine blue stained cerebellar cortex of (2a) group (I) displaying Purkinje cells (P) that house vesicular central nuclei with prominent nucleoli & cytoplasmic Nissl's granules (▶). Notice, pale-stained nuclei of Bergmann astrocytes (B) and crowded deeply stained nuclei of granular cells (G). (2b) group (IV) demonstrating shrunken Purkinje cells (P) having irregular nuclei (black arrow) and depleted cytoplasmic Nissl's granules (▶). Notice: vacuoles (yellow arrow) are present in nearby neuropil. (2c) group (V) demonstrating central vesicular nuclei (black arrow) within Purkinje cells (P). Their cytoplasm studded with Nissl's granules (▶). (2d) group (VI) displaying some Purkinje cells (P) having vesicular nuclei and granular cytoplasm. Others display small irregular shrunken nuclei (black arrow) with few cytoplasmic Nissl's granules (▶). X1000

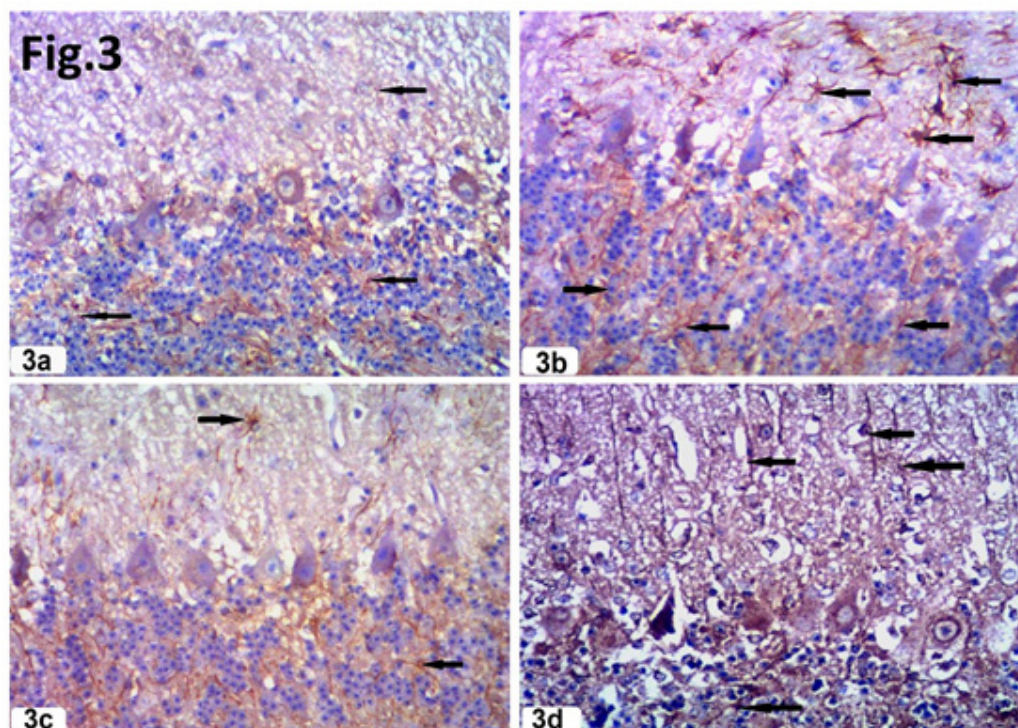


**Fig. 3:** Photomicrographs of GFAP stained cerebellar cortex sections of (3a) group (I) revealing a mild positive reaction to GFAP, with a few dispersed small astrocytes that have short processes (black arrow) in molecular and granular layers. (3b) group (IV) displaying strong GFAP expression with apparently increased size and number of astrocytes (black arrow), having long processes. (3c) group (V) displaying mild to moderate GFAP expression within few cells in molecular and granular layers (black arrow). (3d) group (VI) displaying moderate reaction for GFAP with molecular and granular layers (black arrow). x 200

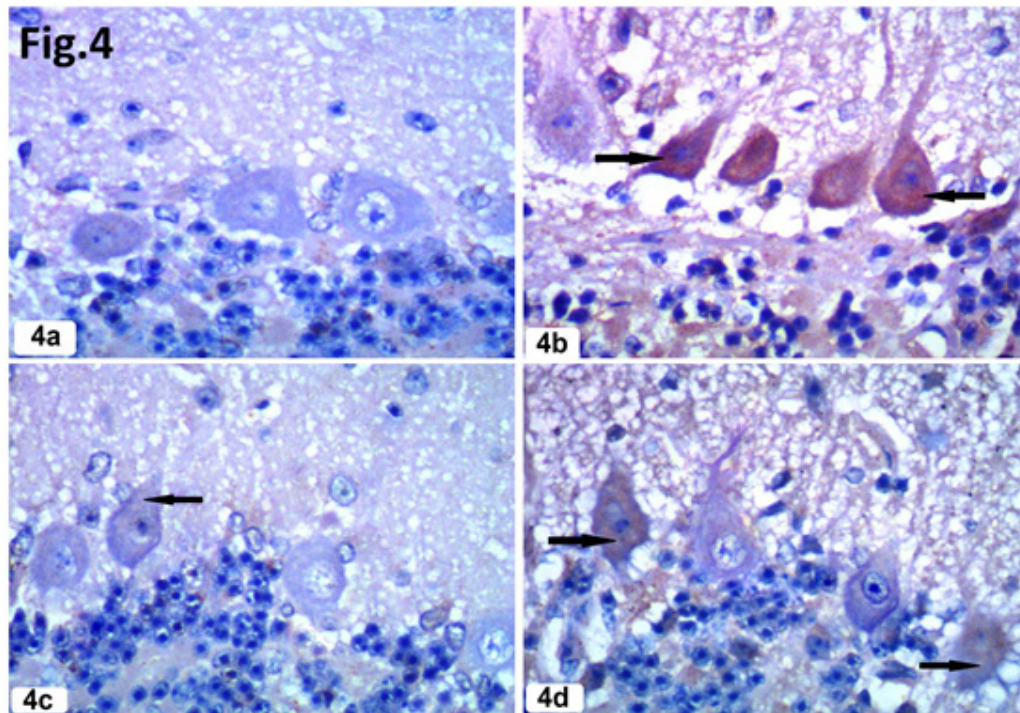


**Fig. 4:** Photomicrographs of INOS stained cerebellar cortex of (4a) group (I) displaying negative iNOS reaction in molecular, Purkinje and granular cell layers. (4b) group (IV) displaying strong, intense iNOS expression in Purkinje cells in the form of brown cytoplasmic staining (black arrow). (4c) group (V) showing none to mild iNOS expression (black arrow) in Purkinje cells. (4d) group (VI) showing moderate reaction for iNOS immunostaining within Purkinje cells (black arrow). x 400

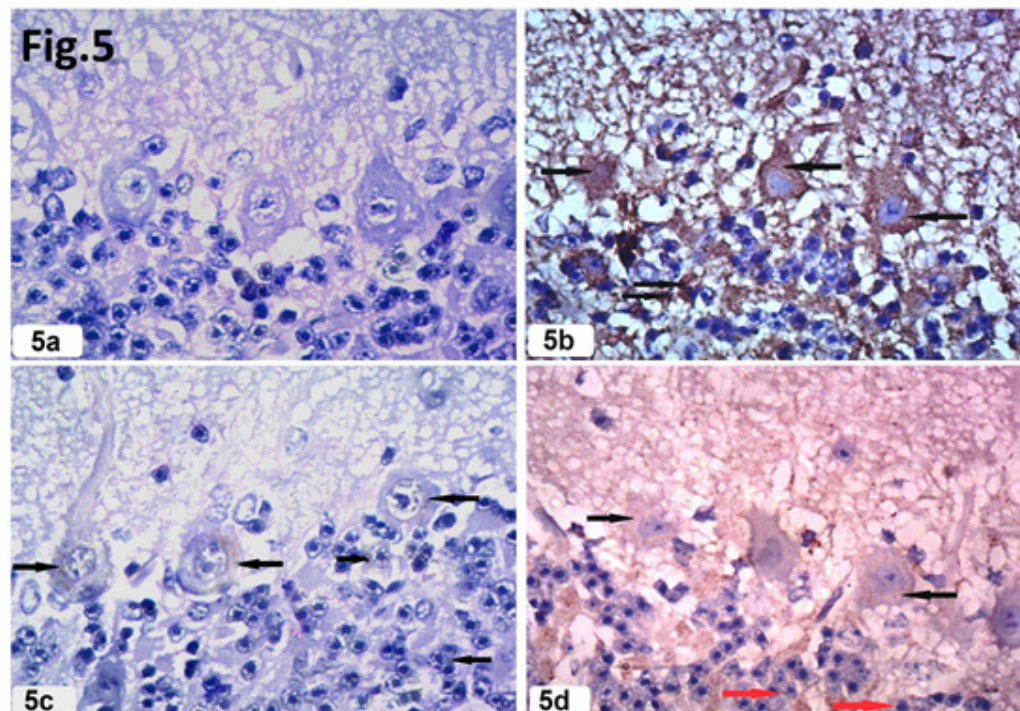


**Fig. 5:** Photomicrographs of caspase 3 stained cerebellar cortex of (5a) group (I) demonstrating negative caspase- 3 cytoplasmic expression in the granule and Purkinje cells. (5b) group (IV) demonstrating strong positive caspase- 3 cytoplasmic expression (black arrow) in granule and Purkinje cells.(5c) group (V) showing negative to weak positive cytoplasmic caspase-3 expression (black arrow) with Purkinje and granule cells.(5d) group (VI) demonstrating moderate caspase-3 cytoplasmic expression (black arrow) in Purkinje cells and mild reaction in granule cells (red arrow). x 400

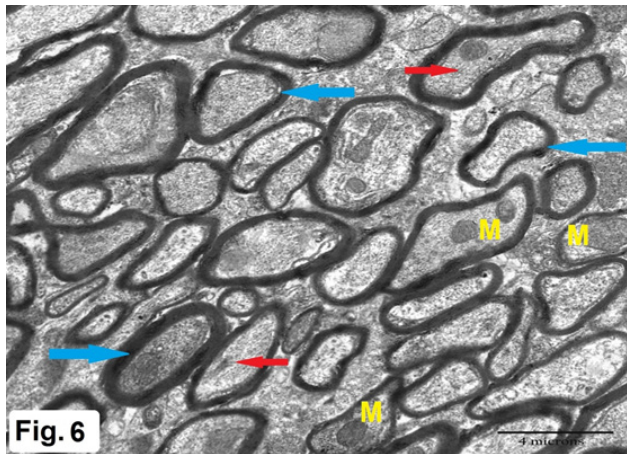


**Fig. 6:** Electron micrograph of molecular layer of control cerebellar cortex group (I) revealing multiple nerve fibers of variable sizes encased in an intact myelin sheath with varying thickness (blue arrows). Mitochondria (M) and microtubules (red arrow) are found in axoplasm. (TEM X 8500)

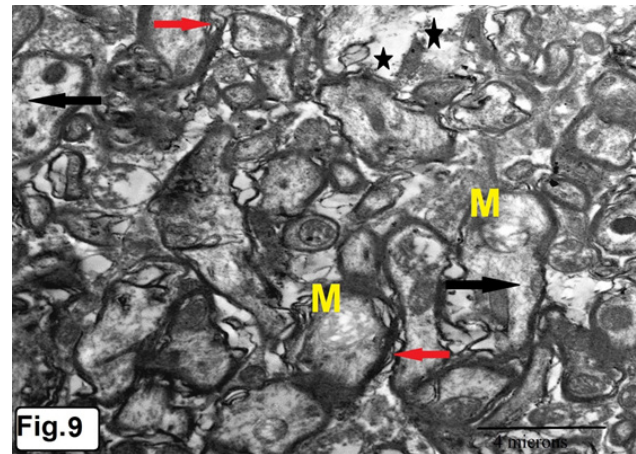


**Fig. 9:** Electron Photomicrograph of molecular layer of sofosbuvir treated cerebellar cortex group (IV) displaying several irregular myelinated nerve fibers having split myelin sheaths (red arrows). Their axoplasm appears rarified (black arrow) housing swollen mitochondria (M) with disrupted cristae. Areas with empty neuropil are noticed (\*). (TEM X 8500)

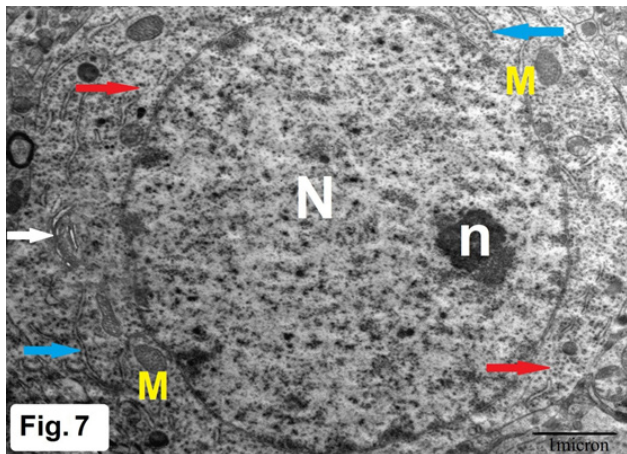


**Fig. 7:** Electron micrograph of Purkinje cell of control cerebellar cortex group (I) displaying euchromatic nucleus (N) and prominent nucleolus (n). Mitochondria (M), multiple rough endoplasmic reticulum cisternae (blue arrow), Golgi apparatus (white arrow), and dispersed ribosomes (red arrow) are seen in cytoplasm. (TEM X 17500)

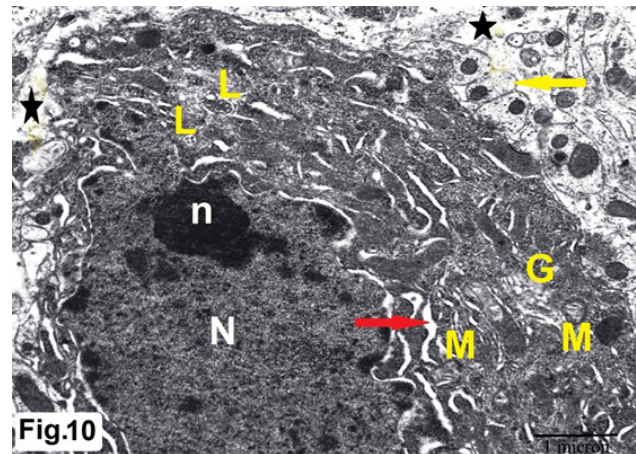


**Fig. 10:** Electron Photomicrograph of Purkinje cell of sofosbuvir treated cerebellar cortex group (IV) demonstrating irregular heterochromatic nucleus (N) with prominent nucleolus (n). The cytoplasm has several dilated rough endoplasmic reticulum cisternae (red arrows), damaged mitochondria (M), disrupted Golgi and 2nd lysosomes (L). The surrounding neuropil appears empty (\*), housing nerve fibers surrounded with thin myelin sheaths (yellow arrow). (TEM X 17500)

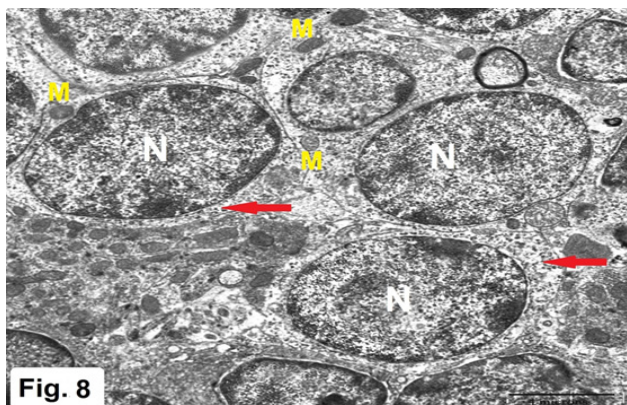


**Fig. 8:** Electron micrograph of granule cells of control cerebellar cortex group (I) displaying euchromatic central nuclei (N) which are encircled by thin rim of cytoplasm housing mitochondria (M) and dispersed free ribosomes (red arrow). (TEM X 8500)

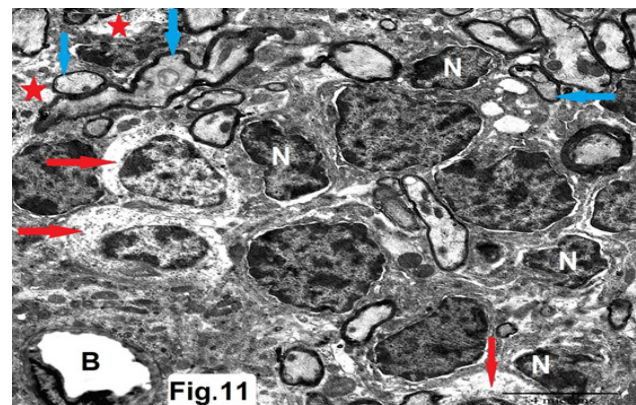


**Fig. 11:** Electron Photomicrograph of granule cells of sofosbuvir treated cerebellar cortex group (IV) displaying irregular, heterochromatic shrunken nuclei (N). Some cells with rarified cytoplasm (red arrow) are present. Irregular shaped nerve fibers with thin myelin sheath (blue arrow) are present among areas of empty neuropil (red star). Dilated blood vessel is noticed (B). (TEM X 8500)

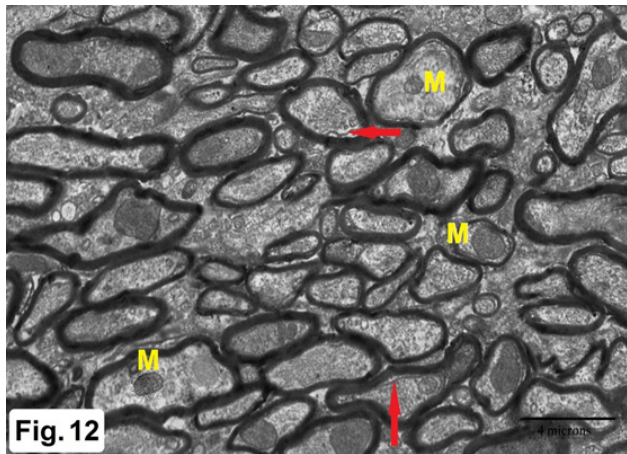


**Fig. 12**

**Fig. 12:** Electron Photomicrograph of molecular layer of cerebellar cortex of sofosbuvir and Mito Q treated group (V) showing multiple nerve fibers surrounded by regular myelin sheath. Their axoplasm shows neurotubules (red arrow) and mitochondria (M). (TEM X 8500)

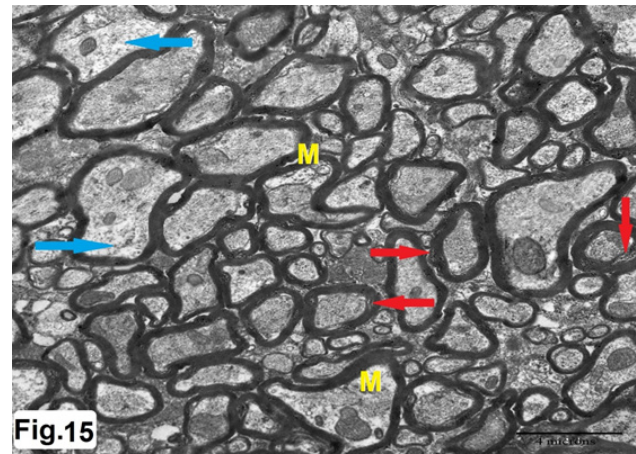


**Fig.15**

**Fig. 15:** Electron Photomicrograph of molecular layer of Sofosbuvir and oxymatrine treated cerebellar cortex group (VI) displaying myelinated nerve fibers encircled by slightly irregular myelin sheath. Some of them exhibit areas of separated myelin sheath (red arrow). Their axoplasm appeared rarified (blue arrow) and has disrupted mitochondria with distorted cristae (M). (TEM X 8500)

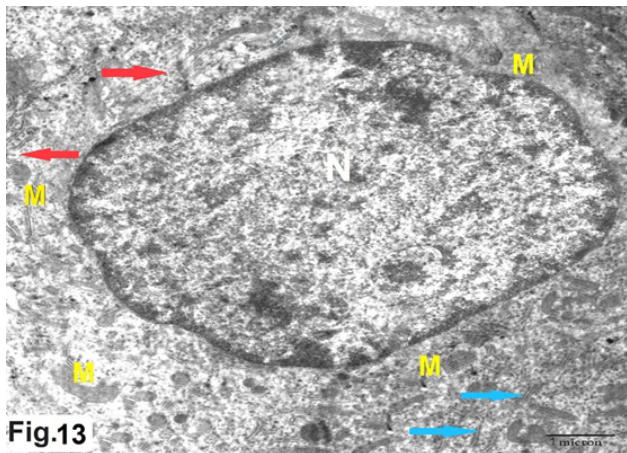


**Fig.13**

**Fig. 13:** Electron Photomicrograph of Purkinje cell of sofosbuvir and Mito Q treated cerebellar cortex group (V) demonstrating euchromatic nucleus (N). Multiple rough endoplasmic reticulum cisternae (blue arrow), free dispersed ribosomes (red arrow) and mitochondria (M) are observed within cytoplasm. (TEM X 17500)

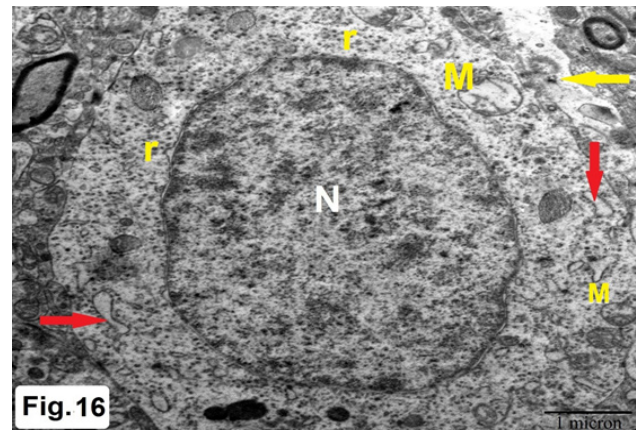


**Fig.16**

**Fig. 16:** Electron Photomicrograph of Purkinje cell of Sofosbuvir and oxymatrine treated cerebellar cortex group (VI) displaying euchromatic nucleus (N). Some dilated rough endoplasmic reticulum cisternae (red arrow), swollen mitochondria with disrupted cristae (M) and multiple free ribosomes (r) are seen in cytoplasm. Notice the empty neuropil (yellow arrow). (TEM X 17500)

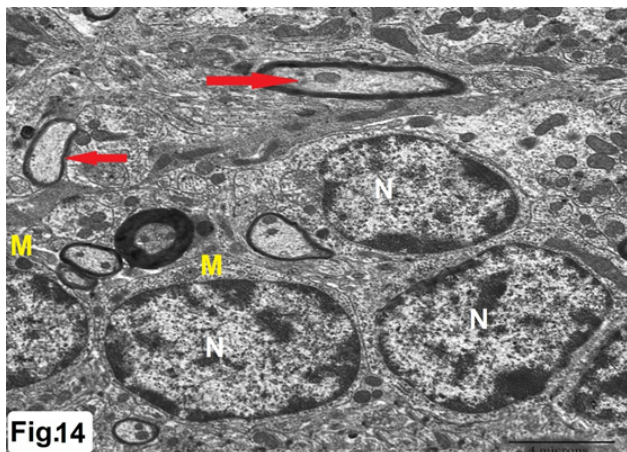


**Fig.14**

**Fig. 14:** Electron Photomicrograph of granule cells of sofosbuvir and Mito Q treated cerebellar cortex group (V) displaying rounded euchromatic nuclei (N) having peripheral heterochromatin clumps encircled by thin rim of cytoplasm having mitochondria (M). Notice: the nearby nerve fibers have mitochondria within their axoplasm and an intact myelin sheath surrounding them (red arrow). (TEM X 8500)

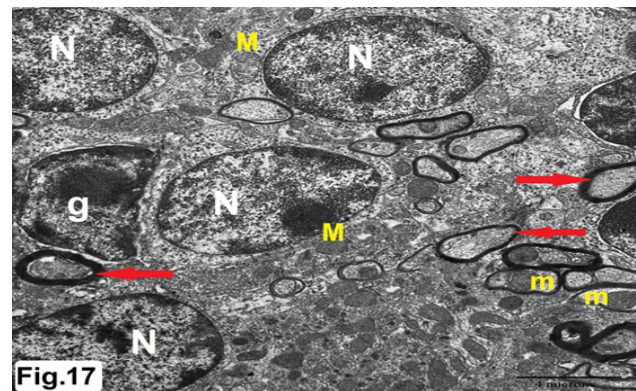


**Fig.17**

**Fig. 17:** Electron Photomicrograph of granule cells of Sofosbuvir and oxymatrine treated cerebellar cortex group (VI) demonstrating rounded euchromatic nuclei having peripheral chromatin clumps (N) encircled by a thin rim of cytoplasm that houses mitochondria (M). Other granule cell (g) appears with irregular, heterochromatic nucleus having wide perinuclear space. The surrounding nerve fibers exhibit intact myelin sheath (red arrow) and mitochondria (m). (TEM X 8500)

Table 1: Mean MDA, GSH and SOD levels within the cerebellar cortical tissue of different groups

Parameters	Mean $\pm$ S D				<i>p</i> – value
	I	IV	V	VI	
MDA ( $\mu\text{mol/g}$ tissue protein)	17.8 $\pm$ 0.4	24.5 $\pm$ 0.4	17.9 $\pm$ 0.3	18.9 $\pm$ 0.5	P1=0.000 P2= 0.344 P3= 0.006 P4=0.000 P5=0.000 P6= 0.037
GSH (Mol/g tissue protein)	46.0 $\pm$ 0.3	34.3 $\pm$ 0.4	45.7 $\pm$ 0.4	44.8 $\pm$ 0.6	P1= 0.000 P2= 0.127 P3= 0.028 P4= 0.000 P5=0.000 P6= 0.021
SOD (U/g of tissue protein)	39.5 $\pm$ 0.2	24.4 $\pm$ 0.6	39.1 $\pm$ 0.5	38.2 $\pm$ 0.4	P1=0.000 P2=0.101 P3=0.003 P4=0.000 P5=0.000 P6=0.018

P1: Comparison was made between group IV and group I.  
P2: Comparison was made between group V and group I.  
P3: Comparison was made between group VI and group I  
P4: Comparison was made between group V and group IV.  
P5: Comparison was made between group VI and group IV.  
P6: Comparison was made between group V and group VI.  
Significance was considered if *P value* < 0.05.  
Highly significance was considered if *P value* > 0.05.  
Non-significance was considered if *P value* < 0.001.

**Table 2:** Mean values regarding molecular layer thickness ( $\mu\text{m}$ ), Granular layer thickness ( $\mu\text{m}$ ), Purkinje cells diameter ( $\mu\text{m}$ ) and Purkinje cells number/ $\text{mm}^2$  of different groups.

Parameters	Mean $\pm$ SD				<i>P</i> – value
	I	IV	V	VI	
Molecular layer thickness ( $\mu\text{m}$ )	186.5 $\pm$ 0.4	134.9 $\pm$ 0.3	186.2 $\pm$ 0.5	185.4 $\pm$ 0.4	P1=0.000 P2=0.132 P3= 0.001 P4=0.000 P5=0.000 P6=0.002
Granular layer thickness ( $\mu\text{m}$ )	136.6 $\pm$ 0.4	121.5 $\pm$ 0.7	136.4 $\pm$ 0.3	135.8 $\pm$ 0.3	P1=0.000 P2=0.100 P3=0.001 P4= 0.000 P5= 0.000 P6= 0.001
Diameter of Purkinje cells ( $\mu\text{m}$ )	273.8 $\pm$ 0.3	177.8 $\pm$ 0.3	273.7 $\pm$ 0.4	271.8 $\pm$ 1.3	P1= 0.000 P2=0.060 P3= 0.001 P4= 0.000 P5= 0.000 P6=0.001
Number of Purkinje cells/ $\text{mm}^2$	6.2 $\pm$ 1.2	2.7 $\pm$ 0.9	6 $\pm$ 1.1	4.9 $\pm$ 0.8	P1= 0.000 P2= 0.532 P3= 0.015 P4= 0.000 P5= 0.000 P6= 0.019

**Table 3:** Mean values regarding area percentage of GFAP, iNos, Caspase-3 immuno-positive reactions in immune-stained sections of different groups

Parameters	Mean ±SD				P – value
	I	IV	V	VI	
Mean area % of GFAP in immune-stained sections	24.8±0.3	42.5±0.4	24.9±0.4	26.4± 1.6	P1=0.000 P2=0.598 P3= 0.008 P4=0.000 P5=0.000 P6=0.011
Mean area % of iNOS in immune-stained sections	1.5±0.2	20.7±0.6	1.8±0.4	2.2± 0.2	P1=0.000 P2=0.139 P3=0.001 P4= 0.000 P5= 0.000 P6= 0.016
Mean area % of Caspase-3 in immune-stained sections	0.3±0.0	34.7±0.5	0.3±0.0	0.5 ± 0.2	P1= 0.000 P2=0.129 P3= 0.004 P4= 0.000 P5= 0.000 P6=0.010

P1: Comparison was made between group IV and control group.

P2: Comparison was made between group V and control group.

P3: Comparison was made between group VI and control group.

P4: Comparison was made between group V and group IV.

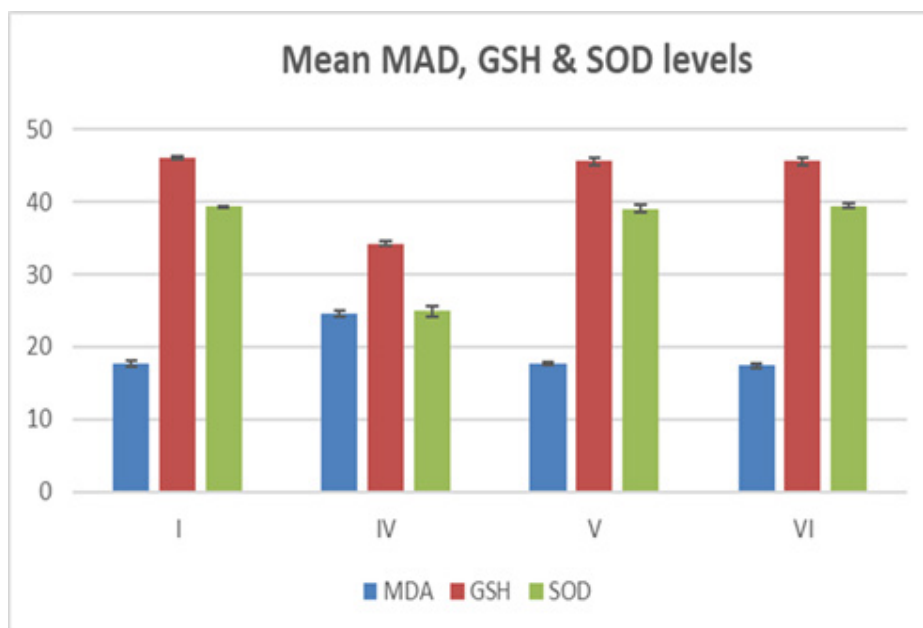
P5: Comparison was made between group VI and group IV.

P6: Comparison was made between group V and group VI.

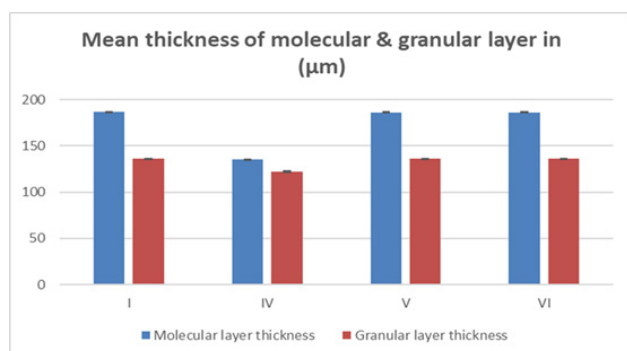
Significance was considered if *P value* < 0.05.

Highly significance was considered if *P value* > 0.05.

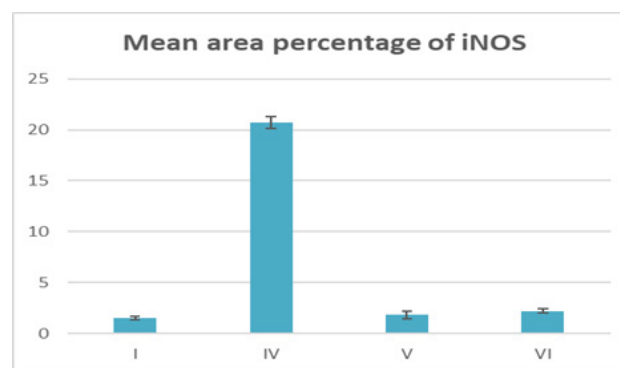
Non-significance was considered if *P value* < 0.001.



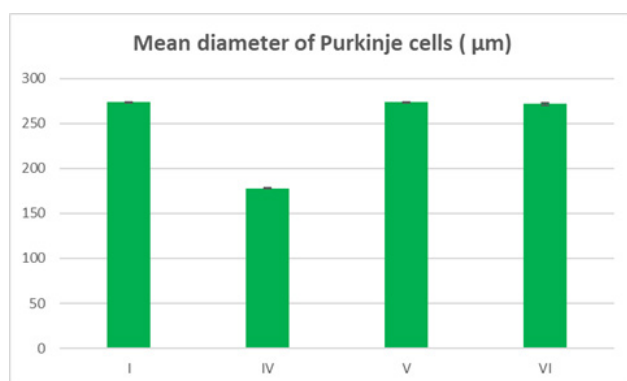
**Histogram 1:** Mean MDA, GSH and SOD levels within the cerebellar cortical tissue of different groups



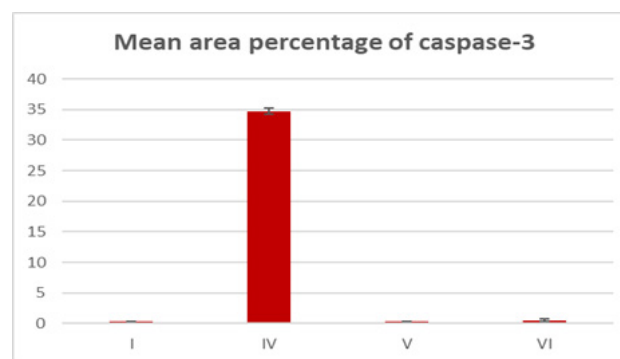
**Histogram 2A:** showing mean molecular and granular layers thickness of various groups



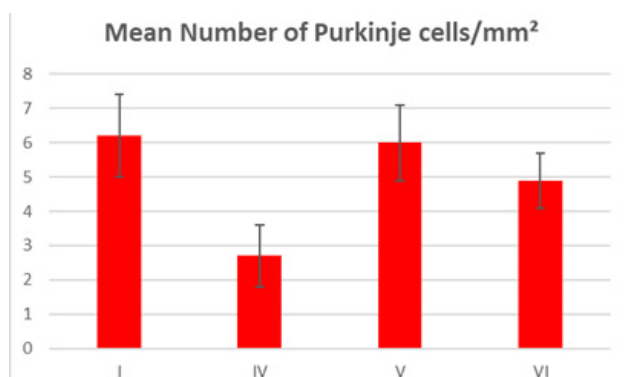
**Histogram 3B:** showing mean area % of iNOS immune-positive reactions within immune-stained sections of different groups



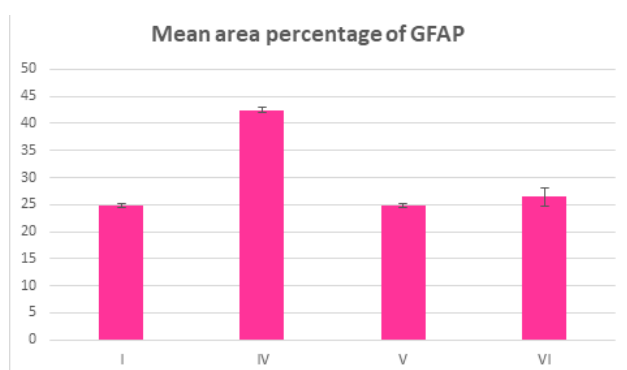
**Histogram 2B:** showing mean diameter of Purkinje cells (µm) of various groups



**Histogram 3C:** showing mean area % of caspase-3 immuno-positive reactions in immune-stained sections of different groups



**Histogram 2C:** showing mean Purkinje cells number /mm² of different groups



**Histogram 3A:** displaying mean area % of GFAP immune-positive within immune-stained sections of different groups

## DISCUSSION

Globally, the primary cause of hepatocellular carcinoma (HCC), liver cirrhosis, chronic liver disease, and hepatic failure is infection with type C hepatitis virus (HCV)<sup>[31]</sup>. Direct-acting anti-viral medications (DAAs), which have more than 90% cure rates, have replaced interferon (IFN)-based treatments, which had 40–70% cure rates, in the anti-viral HCV therapy field<sup>[32]</sup>.

Sofosbuvir-based therapy is the most widely used DAAs treatment. It is orally administrated having low therapeutic failure incidence and high efficacy rate against all HCV genotypes. Furthermore, it has been estimated that using Sofosbuvir may have negative impacts on health as headache, dyspnea, chest distress, muscle spasm, blurred vision, gastrointestinal reflux, and hair loss<sup>[33]</sup>. An earlier study demonstrated that Sofosbuvir treatment results in cerebellar structural degeneration<sup>[4]</sup>. But Limited data is available regarding Sofosbuvir impact on cerebellar cortex. So, that necessitates the aim of this study.

This study's goal was to assess histological, immune-histochemical, and morphometric alterations in adult male albino rats' cerebellar cortex treated with Sofosbuvir and to compare the potential neuroprotective benefits of oxymatrine and mitoquinone (MitoQ) in limiting these alterations.

Histological results of the cerebellar-cortex in group IV receiving Sofosbuvir treatment using light and electron microscopy revealed several histopathological alterations

indicating disrupted structure of cerebellar cortex. Irregular separated myelin sheath surrounding myelinated nerve fibers within molecular layer were noticed. Their axoplasm had degenerated mitochondria. Pyknotic nuclei with perinuclear haloes of cells within molecular layer were also, observed. Purkinje cells appeared disorganized, irregularly arranged, shrunken with irregular outlines. They had hyperchromatic nuclei and vacuolated cytoplasm. Several dilated rough endoplasmic reticulum cisternae, disturbed Golgi apparatus, degenerated Mitochondria and 2<sup>nd</sup> lysosomes were noticed in their cytoplasm. Surrounding neuropil looked rarified. Granular layer cells had shrunken heterochromatic nuclei with widened perinuclear space and rarified cytoplasm. Vascular congestion and extravasation of blood were noticed. Moreover, decrease thickness of both molecular and granular layers, reduction of number and diameter of Purkinje cells were recognized and authenticated by morphometric data analysis. These alterations indicate degeneration of cerebellar cortical neurons following treatment with Sofosbuvir.

These results were in harmony with<sup>[4,33]</sup> who documented degeneration of cerebellar cortical layers and retinal neurons of rats treated with Sofosbuvir respectively. They explained these alterations by pointing out that sofosbuvir, a nucleotide analogue, has a high affinity for mitochondrial polymerases which prevent synthesis of mitochondrial proteins and thereby reduce mitochondrial oxygen consumption. Accordingly, it is suggested that Sofosbuvir damages mitochondria, which causes a huge amount of reactive oxygen species (ROS) to be generated, that is considered as an indicator for oxidative stress. Mitochondrial ROS are thought to be signaling molecules that cause damage to normal tissues by inducing the release of proinflammatory cytokines. Ultrastructural analysis of this group verified the presence of mitochondrial damage within cells of all layers of the cerebellar cortex.

Biochemical results also, confirmed that sofosbuvir's action is mediated through Oxidative stress. Highly significant rise of MDA levels and highly significant decline of GSH and SOD levels within the cerebellar cortical tissues treated with Sofosbuvir in comparison with control group were recorded. This suggests that oxidative stress has been established by high oxidant and low antioxidant levels. Prolonged oxidative stress results in biomacromolecules degradation such as proteins, Lipids, and nucleic acids. ROS causes severe damage to mitochondrial DNA, which in turn increases production of ROS and cause cellular metabolism failure<sup>[34,35]</sup>.

Moreover, some scientists<sup>[36]</sup> reported that brain is more liable to oxidative stress because brain tissues have low antioxidants levels, elevated oxygen consumption rate, and high levels of poly-unsaturated fatty acids.

Prominent peri-neural spaces were noticed around molecular, Purkinje and granule cells. These results were consistent with<sup>[4]</sup>. This could be due to shrinkage of these cells and withdrawal of their processes resulting from

cellular cytoskeleton disintegration that occurs as a result of Sofosbuvir treatment-induced oxidative stress.

Cytoplasmic vacuolation noticed within some Purkinje and granule cells are in harmony with<sup>[6]</sup> who referred this finding to mitochondrial impairment resulting in decreased ATP production and depletion in Na<sup>+</sup>-K<sup>+</sup> pump which cause water to accumulate within the cells to regulate the osmotic pressure. Other researchers<sup>[32]</sup> also, related cytoplasmic vacuolation induced by Sofosbuvir to mitochondrial toxicity. Some scientists<sup>[37]</sup> explained vacuolation of cytoplasm due to disturbed cell membrane function of these cells resulting in increased water and Na<sup>+</sup> ions influx inside these cells.

Within the cells of the cerebellar cortical layers, small darkly stained pyknotic nuclear changes were noticed, which signify apoptosis or programmed cell death. According to a previous study by Abdeen *et al.*, (2020)<sup>[32]</sup>, this might be due to excess ROS production during Sofosbuvir treatment resulting in antioxidant system failure, which leads to oxidative stress.

Regarding vascular congestion and extravasation of red blood cells noticed within cerebellar cortex, similar findings were also reported by Abdeen *et al.*, (2020)<sup>[32]</sup> and El-ghazouly and Yassin, (2021)<sup>[38]</sup>, They observed vascular congestion with extravasated blood within submandibular glands and fundal mucosa of rats treated with Sofosbuvir respectively. This could be related to microcirculatory disturbance with loss of integrity of wall of blood capillaries resulting in blood vessels congestion that is considered as a part of intolerable inflammation. Moreover, in agreement with our results, El Gharabawy *et al.*, (2019)<sup>[39]</sup> reported that Sofosbuvir treatment causes congestion of blood vessels with rat's organs.

Disturbed organization of Purkinje cells noticed on examination of cerebellar cortical sections treated with Sofosbuvir might be due to oxidative stress induced by Sofosbuvir treatment that represents a neuronal insult that triggers an adaptive mechanism in which Purkinje neurons crowd in certain areas in an attempt to restore the connection between different nerve cells, so they can continue functioning as previously documented by<sup>[40]</sup>.

These previous histological findings were enforced by morphometric results that showed a highly significant decrease in thickness of both molecular and granular layers and also, decrease in diameter and number of Purkinje cells compared to control animals.

In the present research, Toluidine blue-stained cerebellar cortical sections from group IV treated with Sofosbuvir showed shrunken Purkinje cells having deeply stained cytoplasm accompanied by a noticeable decrease in the amount of Nissl granules relative to the control group. This finding was consistent with Abdel Mohsen, *et al.*, (2019)<sup>[41]</sup> who observed reduction in cytoplasmic Nissl's granules concentration of Purkinje cells of cerebellum during cisplatin treatment. Other researchers<sup>[42]</sup> explained

this process as chromatolysis which is dissolution of Nissl bodies. This response takes place in neuron's cytoplasm after exposure to trauma or metabolic insults to meet an increased demand for protein synthesis that is required to regenerate damaged neurons.

Other scientists<sup>[43]</sup> related reduction of Nissl's granules content to distribution and dilation of rough endoplasmic reticulum. This might be a result of oxidative stress status occurring with Sofosbuvir treatment in this study. In agreement with this explanation, ultrastructural examination of cerebellar sections treated with Sofosbuvir (group IV) displayed distended cisternae of rough endoplasmic reticulum with Golgi apparatus disruption.

Immunohistochemical staining was applied to confirm these recorded histological and ultrastructural alterations. Sections of the cerebellar cortex stained with GFAP of group IV exhibited several astrocytes with positive immunoreactions. Statistically, its mean area percentage was found to show highly significant increase relative to control animals. This finding was corroborated by Abdel Mohsen, *et al.*, (2019)<sup>[41]</sup> who reported several GFAP positive astrocytes in cerebellar cortex of rats after cisplatin treatment. Increased expression of GFAP in astrocytes may result from hypertrophy and proliferation of astrocytes causing this positive reaction. GFAP is an intermediate filament protein. It is considered a specific marker for mature astrocytes, responsible for keeping their movements and shapes. Additionally, it promotes the central nervous system's synaptic efficiency<sup>[44]</sup>.

The current research results observed a noticeable rise in GFAP level that indicates astrocyte activation. Over-expression of GFAP is a sign for astrogliosis. This reaction can be seen as a compensatory mechanism occurring in CNS injuries due to oxidative stress and excessive production of reactive oxygen species (ROS)<sup>[41,45]</sup>. Other researchers<sup>[46,47]</sup> proposed that any chemical, degenerative, and mechanical injuries to brain cause astrocytes to function as stem cells that start repair sequences. Moreover, astrocytes produce neurotrophic agents, which are critical to neurons' survival.

Regarding inducible nitric oxide synthase (iNOS) immunohistochemical staining, there was a strong positive iNOS immunostaining reaction within Purkinje cells in sections of group IV. Morphometrically, highly significant rise in its mean area-percentage in comparison to control group confirms immunohistochemical result. This was in harmony with<sup>[48]</sup> who reported most of Purkinje cells of cerebellar sections treated with AIC13 displayed strong positive immunoreaction of iNOS. This result indicates that oxidative stress occurred within cerebellar cortex following Sofosbuvir treatment was considered one of mechanisms for neurodegeneration. It is also, explained by Alafify *et al.*, (2021)<sup>[49]</sup> that iNOS over expression usually takes place in oxidative environment. iNOS is a key enzyme for nitric oxide (NO) production, and it plays a vital role in oxidative stress and inflammation<sup>[50]</sup>. Nitric oxide synthase (NOS) enzyme transforms L-arginine into L-citrulline and NO within the cells producing nitric oxide

which is a reactive radical gas. High levels of NO make it more liable to react with superoxide resulting in formation of reactive nitrogen species that is responsible for lipid peroxidation in cell membranes and cell toxicity<sup>[51]</sup>.

Concerning caspase-3 immunostaining, obvious strong positive expression of caspase 3 was recorded within cerebellar cortical sections of group IV treated with sofosbuvir. Morphometrically, highly significant increase in mean area-percentage of caspase-3 within cerebellar cortical sections of group IV in comparison to control animals confirm immunoexpression. Similar findings were observed by Mahran *et al.*, (2022)<sup>[6]</sup>. They reported strong positive expression of caspase-3 within the renal tissue treated with sofosbuvir. Expression of Caspase-3 may be related to oxidative stress caused by Sofosbuvir that results in Mitochondria I damage.

Other researchers<sup>[52]</sup> suggested that high oxidative stress results in increased ROS production that causes mitochondrial disturbance leading to their swelling due to disrupted membrane permeability as well as, increases expression of caspase-3, that triggers apoptosis. Additionally, ROS increases pro-inflammatory cytokines that activate caspase-3, modulating apoptosis, inflammation and finally cellular damage.

Cerebellar cortical sections of group VI treated with Sofosbuvir and oxymatrine showed some improvement. Molecular, Purkinje and granular layers all appeared almost normal. However, molecular layer exhibited some myelinated nerve fibers having slightly irregular, partially separated myelin sheath. Some Purkinje cells had vacuolated cytoplasm and rough endoplasmic reticulum cisternae appeared dilated. These results were confirmed morphometrically by significant decline in thickness of both molecular and granular layers, diameter, and number of Purkinje cells compared to control animals. These results were consistent with<sup>[17]</sup>. They documented that oxymatrine could effectively protect cerebellar cortex from neurotoxic alterations caused by diabetes mellitus.

Oxymatrine (OMT) is a category of major quinolizidine alkaloid, phytochemical agent obtained from the herb *Sophorae Flavescentis Radix* that traditionally grows in China. Chinese medicinal herbs have been extensively utilized in clinical treatment due to their numerous targeting capacity and protective advantages<sup>[53,54]</sup>. Oxymatrine has numerous pharmacological acts, involving anti-inflammatory, anti-viral, anti-apoptotic, anti-oxidative, and anti-immune effects, as a result, it has been used successfully to treat numerous diseases, including chronic hepatitis, bronchial asthma, and several disorders involving ischemia/reperfusion damage in the kidney, liver, intestine, brain and heart<sup>[14]</sup>.

OMT's neuroprotective effects are mainly due to inhibition of oxidative stress, inflammatory response, and cellular apoptosis. Oxymatrine has been demonstrated to decrease pro-inflammatory cytokines, Bcl2 family proteins and toll-like receptor (TLR-4) and nuclear factor-

kappa B (NF- $\kappa$ B) levels as previously reported by other researchers<sup>[55]</sup>.

Some scientists<sup>[56]</sup> related the neuroprotective effects of oxymatrine to its ability to improve the cognitive impairment, reverse neuronal cells damage, and reduction IL-1 $\beta$  and TNF- $\alpha$  release within the nervous tissue. Other scientists demonstrated that oxymatrine improve permeability and integrity blood brain barrier (BBB)<sup>[57]</sup>.

However, Cerebellar sections of group V treated with Sofosbuvir and Mitoquinone showed marked histological, immunohistochemical, and morphometrical improvement. These results were in harmony with Haidar *et al.*, (2022)<sup>[58]</sup> who concluded that mitoquinone has neuroprotective effects in a mouse model of traumatic brain injury.

Mitoquinone (MitoQ), CoQ10 analogue, is a mitochondrial targeted antioxidant molecule. It can permeate blood brain barrier (BBB) and neuronal cell membranes. In contrast to conventional antioxidants, which have difficulty in entering inside mitochondria, MitoQ is concentrated exclusively within the mitochondria, where it performs its local anti-oxidative capacity<sup>[59]</sup>.

MitoQ is produced when a lipophilic triphenylphosphonium cation (TPP<sup>+</sup>) covalently conjugates with ubiquinone or CoQ10 moiety. Because (TPP<sup>+</sup>) has inherent positive charge, it accumulates selectively inside Mitochondria under the influence of high mitochondrial membrane potential as previously reported by Tabet *et al.*, (2022)<sup>[60]</sup>.

MitoQ's quinone moiety is reduced by complex II within the mitochondrial matrix, releasing the corresponding hydroquinone. Hydroquinone is a strong antioxidant that attracts excess reactive oxygen species (ROS), protecting mitochondria electron transport chain from lipid peroxidation and oxidative damage so, preventing cell death<sup>[9]</sup>.

It was recently reported that MitoQ activates nuclear factor erythroid 2-related factor 2 (Nrf2) antioxidant pathway, which has neuroprotective effects against neuronal apoptosis. Superoxide dismutase (SOD), Catalase (CAT), and Glutathione peroxidase 1 (Gpx1) are antioxidant enzyme genes whose expression is increased when Nrf2 pathway activated<sup>[61]</sup>. This is enforced morphometrically in this study by expression of highly significant rise in mean GSH and SOD levels within animals of group V in comparison to group IV.

MitoQ has been proven to be beneficial in exerting powerful antioxidant capacity in alleviating a variety of diseases including neurodegenerative diseases and traumatic brain injury, pressure overload-induced cardiac injury, high fat diet-induced metabolic disorders and diabetic kidney disease. Furthermore, MitoQ also improved disturbance of the blood-brain barrier in subarachnoid haemorrhage in animals, as previously reported by Chen *et al.*, (2020)<sup>[16]</sup> and Reslan *et al.*, (2022)<sup>[62]</sup>.

Other scientists concluded that MitoQ improves neurological and cognitive functions of the brain. It also, has neuroprotective impacts by reducing oxidative stress, neuro-inflammation, and injury of nerve axon. Moreover, it reduces activation of astrocytes and microglia, restoring neuronal and axonal integrity<sup>[58]</sup>.

It is concluded that Sofosbuvir treatment results in noticeable biochemical, histological, immunohistochemical, and morphometrical alterations in the cerebellar cortex of albino male adult rats. The application of Mitoquinone (Mit Q) and oxymatrine as neuroprotective agents enhance these modifications. Utilizing Mitoquinone (Mit Q) resulted in dramatic positive effects. Therefore, we recommend the use of Mitoquinone (Mit Q) as neuroprotective. Its clinical application requires more further studies.

#### CONFLICT OF INTERESTS

There are no conflicts of interest.

#### REFERENCES

- Cheng, P.; Lein-Ray Mo, L.; Chen, C.; Chen, C.; Huang, C. and Kuo, H. (2022):" Sofosbuvir/Velpatasvir for Hepatitis C Virus Infection: Real-World Effectiveness and Safety from a Nationwide Registry in Taiwan". *Infect. Dis. Ther.* 11:485-500. DOI: 10.1007/s40121-021-00576-7.
- Kamal, E.; Asem, N.; Hassany, M.; Elshishiney , G.; Abdel-Razek, W.; Said, H.; Abdel Hamid , S.; Essam, T.; Rehan, A.; Salah, A.; Saad, T.; Shawky, N.; Mostafa, A.; Omar, Y.; Ammar, I.; Saeed, R.; AbdAllah, M.; Jabbour, J.; Hashish, A.; Bastawy, S.; El Qareh, N.; Nahla Gamaleldin, N.; Kabil, K.; Doss, W.; El-Sayed, M.H.; Zaid, H. (2022):"Nationwide hepatitis C virus screening and treatment of adolescents in Egyptian schools". *The Lancet Gastroenterology andhepatology.* Vol. 7:(7):658-665. DOI: 10.1016/S2468-1253(21)00464-7.
- Abdel Ghaffar, T.Y.; El Naghi, S.; Abdel Gawad, M.; Helmy, S.; Abdel Ghaffar, A.; Yousef, M. and Moafy, M. (2019):" Safety and efficacy of combined sofosbuvir/daclatasvir treatment of children and adolescents with chronic hepatitis C Genotype 4". *J. Viral Hepat.* 26:263–270. DOI: 10.1111/jvh.13032.
- Ibrahim, M.A.A.; Sharaf Eldin, H.E. and Elswaidy, N.R. (2021):" Role of aqueous extract of saffron in ameliorating effect of Sofosbuvir on the cerebellar cortex in rat". *Anatomical Record.* 304:714–724. DOI: 10.1002/ar.24501.
- European Association for the Study of the Liver, (2020):" EASL Recommendations on Treatment of Hepatitis C" *J. Hepatology.* 73: 1170 -1218. <https://doi.org/10.1016/j.jhep.2020.08.018>.

6. Mahran, H.A.; Okdah, Y.A.; Zaky, A.A. and Arisha, S.M. (2022): "The possible ameliorative role of *Moringa oleifera* seed oil on sofosbuvir-induced nephrotoxicity in albino rats; histopathological, immunohistochemical and biochemical studies". *The Journal of Basic and Applied Zoology*. 83(16): 1-12. <https://doi.org/10.1186/s41936-022-00281-y>.
7. Hosny, S.A.; Abdel Mohsen, M, A. and Sabry, M.M. (2020): "A Histological Study on the Possible Adverse Effect of Sofosbuvir on Lungs of Adult Male Albino Rats". *Journal of medical histology*. Vol. 4(1): 119-125. DOI: 10.21608/jmh.2020.33529.1077.
8. Mekawy, N. H.; Abdel-aziz, H. M. and Ibrahim, N. E. (2019): "Protective effect of chrysin on corneal structural alterations induced by Sofosbuvir in male albino rats (histological and immunohistochemical study)". *Journal of Histology and Histopathology*. Vol. 6 (5): 1-7. <http://dx.doi.org/10.7243/2055-091X-6-5>.
9. Mao, H.; Zhang, Y.; Xiong, Y; Zhu, Z.; Wang, L. and Liu, X. (2022): "Mitochondria -targeted antioxidant Mitoquinone maintains Mitochondria 1 homeostasis through the sirt3-dependent pathway to mitigate oxidative damage caused by renal ischemia/reperfusion". *Oxidative Medical Cell Longevity*. Article ID:2213503. 18 pages. Doi:10.1155/2022/2213503.
10. Méndez, D.; Arauna, D.; Fuentes, F.; Araya-Maturana, R.; Palomo, I.; Alarcón, M.; Sebastián, D.; Zorzano, A. and Fuentes, E. (2020): "Mitoquinone (MitoQ) Inhibits Platelet Activation Steps by Reducing ROS Levels. *International journal of molecular science*, 21, 6192: 1-12. doi:10.3390/ijms21176192.
11. Fink, B.D.; Liping Yu, Coppey, L.; Obrosof, A.; Shevalye, H.; Kerns, R.J.; Yorek, M.A.; Sivitz, W.I. (2021): "Effect of mitoquinone on liver metabolism and steatosis in obese and diabetic rats. *J. pharmacology research and perspectives*". Vol. 9 (1): 1-9. <https://doi.org/10.1002/prp2.701>.
12. Zhong, L.; Deng, J.; Gu, C.; Shen, L.; Ren, Z.; Ma, X.; Yan, Q.; Deng, J.; Zuo, Z.; Wang, Y.; Cao, S. and Yu, S. (2021): "Protective effect of MitoQ on oxidative stress-mediated senescence of canine bone marrow mesenchymal stem cells via activation of the Nrf2/ARE pathway". In *Vitro Cellular and Developmental Biology*. Animal 57:685–694. <https://doi.org/10.1007/s11626-021-00605-2>.
13. Zhang, G.; Liu, B.; Zeng, Z.; Chen, Q.; Feng, Y.; Ning, X. (2021): "Oxymatrine hydrazone (OMTH) synthesis and its protective effect for rheumatoid arthritis through downregulation of MEK/NF- $\kappa$ B pathway". *Journal of environmental toxicology*. Vol.36 (12): 2448-2453. <https://doi.org/10.1155/2022/24482453>.
14. Lan, X.B.; Ni, Y.S.; Liu, N.; Wei, W.; Liu, Y.; Yang, J.M.; Ma, L.; Bai, R.; Zhang, J. and Yu, J. (2023): "Neuroprotective effects of oxymatrine on hypoxic-ischemic brain damage in neonatal rats by activating the Wnt/ $\beta$ -catenin pathway". *Biomedicine and Pharmacotherapy*. 159 (114266): 1:10. Doi: 10.1016/j.biopha.2023.114266.
15. Huang, Y.P.; Bin He, Song, C.; Long, X. He, J.; Huang, Y. and Liu, L. (2023): "Oxymatrine ameliorates myocardial injury by inhibiting oxidative stress and apoptosis via the Nrf2/HO-1 and JAK/STAT pathways in type 2 diabetic rats". *BMC Complementary Medicine and Therapies*.23(2): 1-13. DOI: 10.1186/s12906-022-03818-4.
16. Chen, X.; Wangb, L. and Songc, X. (2020): "Mitoquinone alleviates vincristine-induced neuropathic pain through inhibiting oxidative stress and apoptosis via the improvement of Mitochondria 1 dysfunction". *Biomedicine and pharmacotherapy*. 125: 110003. <https://doi.org/10.1016/j.biopha.2020.110003>.
17. Shalaby, A.M.; Aboregela, A.M.; Alabiad, M.A. and Sadek, M.T. (2021): "The Effect of Induced Diabetes Mellitus on the Cerebellar Cortex of Adult Male Rat and the Possible Protective Role of Oxymatrine: A Histological, Immunohistochemical and Biochemical Study". *Ultrastructural Pathology*. Vol. 45(3): 182-196. <https://doi.org/10.1080/01913123.2021.1926610>.
18. Shawkat A., Ali Z. and Bashir M. (2023): "Histopathological effect of Sofosbuvir as compared to Sofosbuvir combined with Ribavirin on submandibular salivary glands of adult male albino rats: Histological and immunofluorescent study". *Egyptian Journal of Histology*. 46 (3): 1262-1271. DOI: 10.21608/EJH.2022.124716.1647.
19. Anyakudo, M.M. and Ayibiowu, O.M. (2020): "Comparative Wound Healing Effects of Honey, Olive Oil, Pawpaw Fruit Extract and Iodine in Diabetic Rats: An Evaluation and Prioritization of Potential Alternative Therapeutic Option". *Arch Dia and Obes*. Vol. 2 (5): 224-228. Doi:10.32474/ADO.2020.02.000146.
20. Yeginsu, A. and Ergin, M. (2009): "Antioxidant enzymes and lipid peroxidation in cold ischemic lung preservation". *Experimental and clinical transplantation*. 7(2): 94-98. <https://pubmed.ncbi.nlm.nih.gov/19715512/>.
21. Ganesan, B.; Buddhan, S.; Anandan, R.; Sivakumar, R.; AnbinEzhilan, R. (2010): "Antioxidant defense of betaine against isoprenaline-induced myocardial infarction in rats". *Mol Biol Rep*. (37)1319-1327. <https://doi.org/10.1007/s11033-009-9508-4>.
22. Lu, T. and Finkel, T. (2008): "Free radicals and senescence". *Experimental Cell Research*.314(9):1918-22. <https://doi.org/10.1016/j.yexcr.2008.01.011>.

23. Suvama, K.M.; Layton, C. and Bancroft, J.D. (2019): "Bancroft's Theory and Practice of histological techniques". 8th edition. London: Churchill Livingstone, 173-214.
24. Gokul, S. and Akhil, A. (2012): "Toluidine blue: A review of its chemistry and clinical utility". *J oral Maxillofac. Pathol.* 16(2):251-255. Doi: 10.4103/0973-029x.99081.
25. Saad El-Dien, H.M.; El Gamal, D. A.; Mubarak, H.A. and Samira M. Saleh, S.M. (2010): "Effect of fluoride on rat cerebellar cortex: light and electron microscopic studies" *Egyptian Journal of Histology;* 33(2):245–256.
26. Zhang, J.; Brown, R.P.; Shaw, M.; Vaidya, V.S.; Zhou, Y.; Espandiari, P.; Sadrieh, N.; Stratmeyer, M.; Keenan, J.; Kilty, C.G.; Bonventre, J.V. and Goering, P.L. (2008): "Immunolocalization of Kim- 1, RPA-1, and RPA-2 in kidney of gentamicin-, mercury-, or chromium-treated rats: Relationship to renal distributions of iNOS and nitrotyrosine". *Toxicol. Pathol.;* 36(3):397-409. <https://doi.org/10.1177%2F0192623308315832>.
27. Glamoclijaa, V.; Vilovic, K.; Saraga-Babic, M.; Baranovic, A. and Sapunar, D. (2005):" Apoptosis and active caspase-3 expression in human granulose cells". *American Society for Reproductive Medicine, Fertility and Sterility.* 83(2):426-31. doi: 10.1016/j.fertnstert.2004.06.075.
28. Dykstra, M.J. and Reuss, L.E. (2003):" Staining methods for semi thins and ultra-thins. In: *Biological electron microscopy, theory, techniques and troubleshooting*". 2nd ed. Kluwer Academic Publishers/Plenum Publishers. pp.175- 196.
29. Bozzola, J. J. (2014):" Conventional specimen preparation techniques for transmission electron microscopy of cultured cells". *Methods Mol. Biol.* 1117:1-19.
30. Barton, B. and Peat, J. (2014):" Medical statistics. A Guide to data analysis and critical appraisal". 2nd edition, BMJ Books, Blackwell. 113-119. DOI:10.1002/9780470755945.
31. Shehata, G.A.; Ahmed, G.K.; Hassan, E.A.; Abdel Rehim, A.S.; Mahmoud, S.Z.; Masoud, N. A.; Seifeldein, G.S.; Hassan, W.A. and Aboshaera, K.O. (2022): "Impact of direct-acting antivirals on neuropsychiatric and neurocognitive dysfunction in chronic hepatitis C patients". *The Egyptian Journal of Neurology, Psychiatry and Neurosurgery.* 58(143):1-9. <https://doi.org/10.1186/s41983-022-00568-5>.
32. Abdeen, A. M.; Essawy, T. and Mohammed, S. S. (2020):" Histological and immunohistochemical evaluation to the effect of Sofosbuvir administration on rat's submandibular salivary gland". *Egyptian dental journal for researchers.* Vol. 4 (2): 575-583 <https://www.researchgate.net/publication/349143032>.
33. Elseady, W.S.; Keshk, W.A.; Negm, W.A.; Elkhalawany, W.; Elhanafy, H.; Ibrahim, M.A.A. and Radwan, D.A. (2022):" Saffron extract attenuates sofosbuvir- induced retinal neurodegeneration in albino rats." *Anat Rec.;* 306 (2):422–436. DOI: 10.1002/ar.24942.
34. Issa, N., and El-Sherif, N. (2017): "Histological and Immunohistochemical Studies on the Cornea and Retina of Sofosbuvir Treated Rats". *Austin J Anat* 4(2), 1068. <https://austinpublishinggroup.com/anatomy/fulltext/Anatomy-v4-id1068.php>.
35. Salem, Z.A., Elbaz, D.A. and Farag, D.B.E. (2017):" Effect of an anti-hepatitis c viral drug on rat submandibular salivary gland". *Egyptian dental journal.* 63(1):657-665. <http://dx.doi.org/10.21608/edj.2017.75014>.
36. Farag, E.A. and Yousry, M.M. (2017):" Effect of mobile phone electromagnetic waves on rat testis and the possible ameliorating role of Naringenin: A histological study". *Egyptian Journal of Histology.* 41(1): 108-121. DOI: 10.21608/EJH.2018.7526.
37. Elwan, W. M.; Ragab, A. M. H. and Ragab, M. H. (2018):" Histological and immunohistochemical evaluation of the dose dependent effects of gold nanoparticles on the renal cortex of adult female albino rat". *Egyptian Journal of Histology.* 41(2), 167–181. <https://dx.doi.org/10.21608/EJH.2018.13839>.
38. El-ghazouly, D.E. and Yassin, R.I. (2021):" Effect of Sofosbuvir (Sovaldi) on the Fundic Mucosa of Adult Male Albino Rats and the Possible Protective Role of Fucoidan: Histological, Histochemical, and Immunohistochemical Study". *Egyptian Journal of Histology.* Vol. 45(1): 17-35. <https://dx.doi.org/10.21608/ejh.2021.51729.1392>.
39. El Gharabawy, G. S. H.; Abdallah, E. E. A.; Kaabo, H. F., and Abdel Aleem, A. M. A. (2019):" Histological effects of Sofosbuvir on the kidney of male albino rats and the possible protective role of vitamin C". *The Egyptian Journal of Hospital Medicine,* 76(1), 3335–3354. <https://dx.doi.org/10.21608/ejhm.2019.36898>.
40. Soliman, M.A. and Ali, A.F. (2021):" Comparative Study of the Possible Protective Effects of Omega-3 and Saffron Extract on the Cerebellum of Adult Male Albino Rats Exposed to Cell Phone Electromagnetic Radiations: Histological and Immunohistochemical Study". *Egyptian Journal of Histology.* Vol. 45(1): 208-226. <https://dx.doi.org/10.21608/ejh.2021.59579.1422>.
41. Abdel Mohsen, A.F.; Ahmed, N.A.; Altaib, Z.M. and Zaher, S.M. (2019):" Effect of Cisplatin on Cerebellar Cortex of Albino Rat and Possible Protective Role of Granulocyte Colony Stimulating Factor versus Citrullus Lanatus Juice: A Histological Study". *Egyptian Journal of Histology.* Vol. 43(3): 702-717. <https://dx.doi.org/10.21608/ejh.2019.19193.1197>.

42. Bradley, A.; Bertrand, L.; Rao, D.B.; Hall, D.G. and Sharma, A.K. (2018):" Boorman's Pathology of the rat". 2nd edition. Chapter (13): Brain. 191-215.
43. El-Ghazouly; D. E.; Mahmoud; B. L.; Mansour, M.A. and konsowa, E.B. (2020):" Histological and Immunohistochemical Study on the Effect of Methotrexate on the Cerebellum of Adult Male Albino Rats and The Possible Protective Role of *Lepidium Sativum*". Egyptian Journal of Histology. Vol. 44(1): 241-255. DOI: 10.21608/ejh.2020.23005.1241.
44. Laag, E.M. and Tawfik, S. M. (2021):" Histological Study of the Possible Protective Action of Platelet Rich Plasma on the Injurious Effect Induced by Aluminum Chloride on Albino Male Rat Cerebellar Cortex". Egyptian Journal of Histology. Vol. 44 (4): 1107-1117. <https://dx.doi.org/10.21608/ejh.2021.49889.1386>.
45. El-Azab, N.E.; EL-Mahalaway, A. and Sabry, D. (2018):" Effect of Methyl Mercury on the Cerebellar Cortex of Rats and the Possible Neuroprotective Role of Mesenchymal Stem Cells Conditioned Medium. Histological and Immunohistochemical Study". journal of Stem Cell Research and Therapy. Vol.8 (6): 1-11. DOI: 10.4172/2157-7633.1000430.
46. Dossi, E.; Vasile, F. and Rouach, N. (2018):" Human astrocytes in the diseased brain. Brain Research Bulletin". 136: 139-156. <https://doi.org/10.1016/j.brainresbull.2017.02.001>.
47. Nor-Eldin, E.K. and Elsayed, H. M. (2019):" The possible radioprotective effects of vitamin E, *Nigella sativa* oil, and melatonin against X-ray induced early acute changes in cerebral and cerebellar cortices in Albino rats: Histological and Immunohistochemical". Egyptian journal of histology. Vol. 42 (4): 767-782. <https://dx.doi.org/10.21608/ejh.2019.11113.1106>.
48. Hassan, H.M.; Elnagar, M.R.; Abdelrazik, E.; Mahdi, M.R.; Hamza, E.; Elattar, E.M.; ElNashar, E.M.; Alghamdi, M.A.; Al-Qahtani, Z.; Khulood Mohammed Al-Khater, K.M.; Aldahhan, R.A. and ELdesoqui, M. (2022):" Neuroprotective effect of naringin against cerebellar changes in Alzheimer's disease through modulation of autophagy, oxidative stress and tau expression: An experimental study". Frontiers in Neuroanatomy. Vol.16:1012422, 1-17. <https://doi.org/10.3389/fnana.2022.1012422>.
49. Alafify, A.S.; Wael B. Elkholy, W.B and Noha M. Issa, N. M. (2021):" The Role of *Eruca Sativa* Extract on the Toxic Effect of Proton Pump Inhibitor on Cerebellar Cortex in Adult Males Albino Rat". Egyptian Journal of Histology. Vol.45 (4): 1009-1016. <https://dx.doi.org/10.21608/ejh.2021.78909.1500>.
50. Abd El Fattah, E.R.; Abd El Fattah, M.T. and EL-Bestawy, E.M. (2021):" Possible Protective Role of L-Carnitine Against Hyperthyroidism Induced Osteoporotic Changes in Femoral Diaphysis of Adult Male Albino Rats". Egyptian Journal of Histology. Vol.46 (1): 91-104. <https://dx.doi.org/10.21608/ejh.2021.86696.1528>.
51. Yassien, R.I.; Zedan, O.I.I. and Ghoneim, N.S. (2020):" Histological and Immunohistochemical Study on the Effect of Sodium iodate on the Retina of Adult Male Albino Rat and the Possible Protective Role of Silymarin". Egyptian Journal of Histology. Vol. 44(4): 961-978. <https://dx.doi.org/10.21608/ejh.2020.46113.1373>.
52. Refaie, M. M.; Ibrahim, S. A.; Sadek, S. A. and Abdelrahman, A. M. (2017). Role of ketotifen in methotrexate-induced nephrotoxicity in rats. Egyptian Journal of Basic and Clinical Pharmacology. Vol. 7(2), 70-80. DOI:10.32527/2017/101427.
53. Li, J.; Liang, J.; Zeng, M.; Sun, K.; Luo, Y.; Zheng, H.; Li, F.; Yuan, W.; Hongwei Zhou, H.; Liu, J. and Sun, H. (2022):" Oxymatrine ameliorates white matter injury by modulating gut microbiota after intracerebral hemorrhage in mice". CNS Neurosci Ther. 29 (Suppl.1):18-30. DOI: 10.1111/cns.14066.
54. Han, X.; Ma, T.; Wang, Q.; Jin, C.; Yusheng Han, Y; Liu, G. and Li, H. (2023):" The mechanism of oxymatrine on atopic dermatitis in mice based on SOCS1/JAK-STAT3 pathway". Frontiers in Pharmacology. 1-8. <https://doi.org/10.3389/fphar.2022.1091090>.
55. Guan, B.; Chen, R.; Zhong, M.; Liu, N. and Qin Chen, Q. (2020):" Protective effect of Oxymatrine against acute spinal cord injury in rats via modulating oxidative stress, inflammation and apoptosis". Metabolic Brain Disease. 35: 149-157. <https://doi.org/10.1007/s11011-019-00528-8>.
56. Dong, PL.; Li, ZQ.; Teng, CI.; Yin, X.; Cao, XK.; Hua Han, H. (2021):" Synthesis and evolution of neuroprotective effects of oxymatrine derivatives as anti-Alzheimer's disease agents". Chem. Biol. Drug. Des. 98:175-181. DOI: 10.1111/cbdd.13862.
57. Yu, J; Liu, Q.; Li, X; Zhao, M.; Sun, T.; Hu, N.; Jiang, W; Zhang, R.; Yang, P. and Yang, Q. (2020):" Oxymatrine Improves the Integrity of the Blood Brain Barrier after Cerebral Ischemia-Reperfusion Injury through the Caveolin-1/MMP-9 Signalling Pathway". Research square. 1:23. <https://doi.org/10.21203/rs.3.rs-116504/v1>.
58. Haidar, M.A.; Shakkour, Z.; Barsa, C.; Tabet, M.; Mekhjian, S.; Darwish, H.; Goli, M.; Shear, D.; Pandya, J.D.; Mechref, Y.; El Khoury, R.; Wang, K. and Kobeissy, F. (2022):" Article Mitoquinone Helps Combat the Neurological, Cognitive, and Molecular Consequences of Open Head Traumatic Brain Injury at Chronic Time Point". Biomedicines. 10(2), 250: 1-23. <https://doi.org/10.3390/biomedicines10020250>.
-

59. Ismail, H.; Shakkour, Z.; Tabet, M.; Abdelhady, S.; Kobaisi, A.; Abedi, R.; Nasrallah, L.; Pintus, G.; Al-Dhaheri, Y.; Mondello, S.; El-Khoury, R.; Eid, A.H.; Kobeissy, F. and Salameh, J. (2020): "Traumatic Brain Injury: Oxidative Stress and Novel Anti-Oxidants Such as Mitoquinone and Edaravone". *Antioxidants*. 9 (10):943 (1-18). doi: 10.3390/antiox9100943.
60. Tabet, M.; El-Kurdi, M.; Haidar, M.A.; Nasrallah, L.; Reslan, M.A.; Shear, D.; Pandya, J.D.; El-Yazbi, A.F.; Sabra, M.; Mondello, S.; Mechref, Y.; Shaito, A.; Wang, K.K.; El-Khoury, R. and Kobeissy, F. (2022): "Mitoquinone supplementation alleviates oxidative stress and pathologic outcomes following repetitive mild traumatic brain injury at a chronic time point". *Exp Neurol*. 351:113987. doi: 10.1016/j.expneurol.2022.113987.
61. Cores, A.; Carmona-Zafra, N.; Clerigué, J.; Villacampa, M.; J Carlos Menéndez, J.C. (2023): "Quinones as Neuroprotective Agents". *Antioxidants (Basel)*, 12(7):1464. doi: 10.3390/antiox12071464.
62. Reslan, M.A.; Jammoul, M.; Nasrallah, L.; Tabet, M.; El-Kurdi, M.; Mekhjian, S.; Nwaiwu, J.; Goli, M.; Mechref, Y.; Wang, K.K.; Kobeissy, F. and El Khoury, R. (2022): "Neurological Outcomes Following Mitoquinone Supplementation in Mice, 3 and 7 Days Post Repeated Mild Traumatic Brain Injury". *preprints.org*. Social sciences. Cognitive science. Article ID: 2022070316. <https://doi.org/10.20944/preprints202207.0316.v1>.

## الملخص العربي

## دراسة هستولوجية لمقارنة التأثير الوقائي المحتمل للميتوكينون مقابل الأوكسيماترين على قشرة المخيخ لذكور الجرذان البيضاء البالغة المعالجة بالسوفوسبوفير

مني عبد المولي سليمان و رانيا سعيد عمارة و داليا عبد الرازق نوية

قسم الهستولوجيا و بيولوجيا الخلية- كلية الطب- جامعة المنوفية

**المقدمة:** يعتبر التهاب الكبدى الوبائي المزمن من قضايا الصحة العامة في جميع أنحاء العالم. ويعتبر السبب الرئيسي للوفيات المرتبطة بالكبد. لقد أحدث عقار سوفوسبوفير، وهو دواء ذو تأثير مباشر مضاد للفيروسات، ثورة في علاج فيروس التهاب الكبدى الوبائي بمعدل نجاح مرتفع. ومع ذلك، فإن تأثيره على المخيخ لا يزال غير واضح. الميتوكينون والأوكسيماترين لهما تأثيرات وقائية علي الجهاز العصبي.

**الهدف من البحث:** يهدف الى تقييم الفوائد الوقائية العصبية للميتوكينون مقابل الأوكسيماترين ضد التغيرات المستحدثة على قشرة المخيخ لذكور الجرذان البيضاء المعالجة بالسوفوسبوفير.

**المواد والطرق :** تم تقسيم ستة وسبعون جرذاً بالغاً من ذكور الجرذان البيضاء إلى ست مجموعات، المجموعة الأولى (١٦ جرذاً) خدمت كمجموعة ضابطة، المجموعة الثانية (١٢ جرذاً) والثالثة (١٢ جرذاً) (المجموعة المعالجة بالميتو كوينون والأوكسيماترين على التوالي)، المجموعة الرابعة (١٢ جرذاً) (المجموعة المعالجة بالسوفوسبوفير)، المجموعة الخامسة (١٢ جرذاً) (المجموعة المعالجة بالسوفوسبوفير والميتو كوينون)، المجموعة السادسة (١٢ جرذاً) (المجموعة المعالجة بالسوفوسبوفير وأوكسيماترين). و في نهاية الدراسة تم استخراج المخيخ و معالجته للدراسات الكيميائية و الهستولوجية و الهستوكيميائية المناعية (البروتين الليفى الحامضى(GFAP) وسينسيز أكسيد النيتريك المحفز (iNOS) و كسباس (3-Caspase) و الدراسات المجهرية الإلكترونية، كما تم إجراء الدراسات المورفومترية .

**النتائج:** أظهر العلاج بالسوفوسبوفير تغييراً في تركيب قشرة المخيخ. أظهرت الطبقة الجزيئية فراغات حول خلاياها العصبية مع وجود شقوق في أغشية الميلين التي تغلف الألياف العصبية. علاوة على ذلك، فقد ظهرت خلايا البركينجى منكمشة و غير منظمة و ذات انوية داكنة و فقدت حبيبات نيسل . و قد ظهرت بعض الخلايا الصغيرة الضامرة في الطبقة الحبيبية. كما لوحظ وجود زيادة كبيرة في التفاعل المناعى للبروتين الليفى الحامضى(GFAP) و لسينسيز أكسيد النيتريك المحفز(iNOS) و لكسباس 3(Caspase-3).

كما أظهرت النتائج ان تناول ميتوكوينون (ميتو كيو) والأوكسيماترين أدى إلى تحسين هذه التغييرات. و أن الميتوكوينون (ميتو كيو) له حماية عصبية أفضل ضد التغيرات الهستولوجية في قشرة المخيخ المعالجة بالسوفوسبوفير.

**الاستنتاج:** العلاج بالسوفوسبوفير يسبب تغيرات هستولوجية و هستوكيميائية مناعية في قشرة المخيخ لذكور الجرذان البيضاء البالغة. و أن الميتوكوينون له تأثير وقائى أفضل من الأوكسيماترين ضد هذه التغييرات .